HAL open science

An extension of the Crouzeix-Raviart space to general meshes with application to quasi-incompressible linear elasticity and Stokes flow

Daniele Antonio Di Pietro, Simon Lemaire

To cite this version:

Daniele Antonio Di Pietro, Simon Lemaire. An extension of the Crouzeix-Raviart space to general meshes with application to quasi-incompressible linear elasticity and Stokes flow. Mathematics of Computation, 2014, Published online, pp.31. 10.1090/S0025-5718-2014-02861-5 . hal-00753660v3

HAL Id: hal-00753660

https://hal.science/hal-00753660v3

Submitted on 6 Jun 2013 (v3), last revised 1 Oct 2014 (v4)

HAL is a multi-disciplinary open access archive for the deposit and dissemination of scientific research documents, whether they are published or not. The documents may come from teaching and research institutions in France or abroad, or from public or private research centers.

L'archive ouverte pluridisciplinaire **HAL**, est destinée au dépôt et à la diffusion de documents scientifiques de niveau recherche, publiés ou non, émanant des établissements d'enseignement et de recherche français ou étrangers, des laboratoires publics ou privés.

An extension of the Crouzeix–Raviart space to general meshes with application to quasi-incompressible linear elasticity and Stokes flow

Daniele A. Di Pietro*[1] and Simon Lemaire†[2]

[1] Université Montpellier 2, I3M, 34057 Montpellier CEDEX 5, France
[2] IFP Énergies nouvelles, Department of Applied Mathematics, 1 & 4 avenue de Bois-Préau, 92852 Rueil-Malmaison CEDEX, France

June 5, 2013

Abstract

In this work we introduce a discrete functional space on general polygonal or polyhedral meshes which mimics two important properties of the standard Crouzeix–Raviart space, namely the continuity of mean values at interfaces and the existence of an interpolator which preserves the mean value of the gradient inside each element. The construction borrows ideas from both Cell Centered Galerkin and Hybrid Finite Volume methods. The discrete function space is defined from cell and face unknowns by introducing a suitable piecewise affine reconstruction on a (fictitious) pyramidal subdivision of the original mesh. Two applications are considered in which the discrete space plays an important role, namely (i) the design of a locking-free primal (as opposed to mixed) method for quasi-incompressible planar elasticity on general polygonal meshes; (ii) the design of an inf-sup stable method for the Stokes equations on general polygonal or polyhedral meshes. In this context, we also propose a general modification, applicable to any suitable discretization, which guarantees that the velocity approximation is unaffected by the presence of large irrotational body forces provided a Helmholtz decomposition of the right-hand side is available.The relation between the proposed methods and classical finite volume and finite element schemes on standard meshes is investigated. Finally, similar ideas are exploited to mimic key properties of the lowest-order Raviart–Thomas space on general polygonal or polyhedral meshes.
Mathematics Subjects Classification. 65N08, 65N30, 74B05, 76D07

1 Introduction

In the context of industrial simulators, lowest-order methods for diffusive problems on general polygonal or polyhedral meshes have received an increasing attention over the last few years. The reasons are multifold. Using general polyhedral elements may ease the discretization of complex domains, and disposing of discretization methods applicable to general meshes is mandatory whenever the user cannot adapt the mesh to the needs of the numerical scheme. This is the case, e.g., in the context of computational geosciences, where the discretization of the subsoil is developed in a separate stage, and is focused on integrating physical and geometric data resulting from the seismic analysis. Fairly general meshes can thus be encountered,

*Daniele.Di-Pietro@univ-montp2.fr
†Corresponding author, simon.lemaire@ifpen.fr

featuring, e.g., nonmatching interfaces corresponding to geological faults or general polyhedral elements resulting from the degeneration of hexahedral cells in eroded layers. Polyhedral elements may additionally be present in near wellbore regions, where the use of radial meshes can be prompted by (qualitative) a priori knowledge of the solution. Nonconforming h-refinement can also appear at specific locations where the resolution needs to be increased, or when moving fronts are present. In this context, the use of lowest-order methods is justified both by the inherent uncertainty associated to physical data and the need to keep computational costs within affordable bounds.

Among the methods that have appeared in recent years, the most directly related to the present work are the Mimetic Finite Difference (MFD) method of Brezzi, Lipnikov et al. [13, 11, 12], the Hybrid Finite Volume (HFV) method of Eymard, Gallouët and Herbin [25], and the Mixed Finite Volume (MFV) method of Droniou and Eymard [20]. The close relation among these methods has recently been investigated in [22]. The main result of the present work is the construction of a discrete space of piecewise affine functions which extends two important properties of the classical Crouzeix–Raviart space [15] to general meshes, namely,

(CR1) the continuity of mean values at interfaces. Since we deal with piecewise affine functions, this property is equivalent to the continuity at face barycenters;

(CR2) the existence of an interpolator which preserves the mean value of the gradient inside each element. Such interpolator can play the role of a Fortin operator [10].

Let $\mathcal{K}_h$ denote a general polygonal or polyhedral mesh of the bounded domain Ω matching the regularity requirements discussed in Section 2. In the spirit of Cell Centered Galerkin (ccG) methods [16], the discrete space is constructed in three steps:

(i) we fix the vector space $\mathbb{V}_h$ of face- and cell-centered degrees of freedom (DOFs) on $\mathcal{K}_h$;

(ii) we define a discrete gradient reconstruction operator $\mathfrak{G}_h$ acting on $\mathbb{V}_h$. The reconstructed gradient is piecewise constant on a fictitious pyramidal submesh $\mathcal{P}_h$ obtained by subdividing each element using one interior point (the cell center), and it results from the sum of two terms: a consistent part depending on face unknowns only plus a subgrid correction involving both face and cell unknowns. The continuity of mean values at interfaces is ensured by finely tuning the latter contribution;

(iii) we define an affine reconstruction operator $\mathfrak{R}_h$ acting on $\mathbb{V}_h$ which maps every vector of DOFs on a broken affine function on $\mathcal{P}_h$. This function is obtained by perturbing the (unique) face unknown associated to each pyramid with a linear correction based on the discrete gradient $\mathfrak{G}_h$. The discrete space is then defined as

$$\mathfrak{CR}(\mathcal{K}_h) := \mathfrak{R}_h(\mathbb{V}_h) \subset \mathbb{P}_d^1(\mathcal{P}_h),$$

with $\mathbb{P}_d^1(\mathcal{P}_h)$ space of broken affine functions on $\mathcal{P}_h$, cf. (4).

The pyramidal submesh is fictitious in the sense that all the relevant geometric information can be computed on the primal mesh, which is therefore the only one that needs to be described and manipulated by the end-user. In Appendix A, similar ideas are used to construct a $\boldsymbol{H}(\mathrm{div};\Omega)$-conforming discrete space on general meshes which mimics two key properties of the standard lowest-order Raviart–Thomas space, namely the (full) continuity of normal values at interfaces and the approximation of vector-valued fields. We mention at this point the recent work of Vohralík and Wohlmuth [34, 35] which proposes efficient implementation strategies for classical nonconforming and mixed finite element approximations of diffusive problems, and addresses general meshes with a different approach.

The first application we consider is linear elasticity, which was also the original motivation for this work. Our main result is the design of a primal (as opposed to mixed) method based on the space $\mathfrak{CR}(\mathcal{K}_h)$ (and thus applicable to general meshes) which is locking-free in the quasi-incompressible limit in two space dimensions (the required regularity estimate for the continuous solution is still an open problem in higher space dimensions).

It has been long known that the accuracy of lowest-order H^1-conforming (Lagrange) finite element approximations deteriorates when quasi-incompressible materials are considered, i.e., for large values of the first Lamé parameter λ; cf., e.g., [8, Section 11.3]. This is a consequence of the fact that the convergence estimates are not uniform in λ, which, in turn, reflects the inability of the discretization space to accurately represent nontrivial solenoidal fields. One classical way of circumventing this problem is the use of mixed formulations, resulting in methods which converge uniformly in λ, but which are often computationally more expensive than primal methods. Examples include the PEERS method of Arnold, Brezzi and Douglas [2], the mixed method of Stenberg [31], and the mixed methods of Chavan, Lamichhane and Wohlmuth [14], and Lamichhane and Stephan [30]. All these methods require matching triangular or quadrilateral meshes. General meshes similar to the ones addressed in this work have been recently considered by Beirão da Veiga [3], who introduces a mixed MFD method which does not lock in the quasi-incompressible limit.

The problem of locking has also been addressed without resorting to mixed formulations, and several methods can be found in the literature. On matching triangular meshes, we can cite, e.g., the p-version method of Vogelius [33], and the nonconforming methods of Falk [26]. Concerning general meshes, we mention the very recent work of Beirão da Veiga, Brezzi, and Marini [4] on virtual elements for linear elasticity. In the MFD framework, we cite the method for the two-dimensional Stokes problem proposed by Beirão da Veiga, Gyrya et al. [5], whose analysis and extension to three space dimensions have been considered in [6]. In both cases the authors consider a (possibly fourth-order) tensor viscosity, which allows an extension to linear elasticity. We note, moreover, that inf-sup stable mixed methods for the Stokes problem can be, whenever the pressure is discontinuous, converted to a locking-free primal method for the pure displacement linear elasticity problem by static condensation of pressures. This strategy can be applied to the method of [5, 6]. In the MFV framework, we can cite the work of Droniou and Eymard [21], where the Stokes problem is also addressed.In this work we take inspiration from the classical Crouzeix–Raviart method of Brenner and Sung [9]. Here, while property (CR1) ensures adequate conformity properties to the space, property (CR2) plays an important role in deriving an error estimate uniform in λ. Another source of inspiration is the work of Hansbo and Larson [28, 29], where a locking-free Discontinuous Galerkin (dG) method on matching triangular meshes is analyzed; see also Di Pietro and Nicaise [19] for an extension to composite materials. Coercivity is here ensured by a least-square penalization of interface jumps. In our method, a similar device is required in the case of mixed type boundary conditions to invoke a discrete Korn's inequality on broken polynomial spaces [7]. For the pure displacement problem, the naturally coercive Navier–Cauchy formulation allows to circumvent the use of Korn's inequality. Up to a suitable treatment of the right-hand side, it is possible to prove for our scheme a local conservation property similar to finite volume methods. In this case, the face unknowns act as Lagrange multipliers associated to the flux continuity constraint. Yet another treatment of the right-hand side allows to recover the method of [9] on matching simplicial meshes.

As a second, closely related application, we propose an inf-sup stable method for the Stokes problem. Taking inspiration from the recent work of Galvin, Linke et al. [27], we additionally consider the problem of large irrotational body forces and pinpoint a strategy to preserve accuracy in the approximation of the velocity field for the case when a Helmholtz decomposition

of volumetric body forces is available. We emphasize that this strategy is applicable to more general discretizations than the one considered in this work.Also in this case, suitable modifications of the right-hand side allow to establish a link with finite volumes, and nonconforming finite element methods on matching simplicial meshes.

The paper is organized as follows. In Section 2 we introduce the notation and define the concepts of admissible mesh sequence and pyramidal submesh inspired by [17, 16]. The main novelty of this section is the proof that the pyramidal submesh inherits the shape- and contact-regularity properties of the original mesh. Section 3 details the construction of the space $\mathfrak{CR}(\mathcal{K}_h)$ as well as the proofs of the properties (CR1) and (CR2). In Section 4 we present two applications of the space $\mathfrak{CR}(\mathcal{K}_h)$, namely the approximation of the linear elasticity problem for quasi-incompressible materials and the discretization of the Stokes equations with large irrotational body forces. Finally, in Appendix A we adapt the ideas of Section 3 to construct a discrete space which mimics the properties of the lowest-order Raviart–Thomas space on general polygonal or polyhedral meshes.

2 Admissible mesh sequences

Following [17, Chapter 1] and [16, Section 1], we introduce in this section the concept of admissible mesh sequence of a bounded connected polygonal or polyhedral domain $\Omega \subset \mathbb{R}^d$, $d \geqslant 2$. For the sake of brevity, we only give the proofs of the new results, and refer to [17, 16] for further details.

2.1 Shape- and contact-regularity

Let $\mathcal{H} \subset \mathbb{R}_*^+$ denote a countable set having 0 as its unique accumulation point. We consider mesh sequences $\mathcal{K}_\mathcal{H} := (\mathcal{K}_h)_{h\in\mathcal{H}}$ where, for all $h \in \mathcal{H}$, $\mathcal{K}_h$ denotes a finite collection of nonempty disjoint open polyhedra $\mathcal{K}_h = \{K\}$ such that $\overline{\Omega} = \bigcup_{K\in\mathcal{K}_h} \overline{K}$ and $h = \max_{K\in\mathcal{K}_h} h_K$ (h_K denotes here the diameter of the element $K \in \mathcal{K}_h$). We say that a hyperplanar closed connected subset F of $\overline{\Omega}$ is a mesh face if it has positive $(d-1)$-dimensional measure and if either there exist $K_1, K_2 \in \mathcal{K}_h$ such that $F \subset \partial K_1 \cap \partial K_2$ (and F is called an interface) or there exists $K \in \mathcal{K}_h$ such that $F \subset \partial K \cap \partial\Omega$ (and F is called a boundary face). Interfaces are collected in the set $\mathcal{F}^{\mathrm{i}}_{\mathcal{K}_h}$, boundary faces in $\mathcal{F}^{\mathrm{b}}_{\mathcal{K}_h}$ and we let $\mathcal{F}_{\mathcal{K}_h} := \mathcal{F}^{\mathrm{i}}_{\mathcal{K}_h} \cup \mathcal{F}^{\mathrm{b}}_{\mathcal{K}_h}$. The diameter of a face $F \in \mathcal{F}_{\mathcal{K}_h}$, is denoted by h_F. Moreover, we set, for all $K \in \mathcal{K}_h$, $\mathcal{F}_K := \{F \in \mathcal{F}_{\mathcal{K}_h} \mid F \subset \partial K\}$. According to the context, the notation $|\cdot|$ is used for the d- or the $(d-1)$-dimensional Lebesgue measure. In the rest of this section, we discuss some fairly general regularity conditions on the mesh sequence $\mathcal{K}_\mathcal{H}$ that allow to prove basic results such as trace and inverse inequalities and polynomial approximation properties.

Definition 1 (Shape- and contact-regularity)**.** *The mesh sequence $\mathcal{K}_\mathcal{H}$ is shape- and contact-regular if for all $h \in \mathcal{H}$, $\mathcal{K}_h$ admits a matching simplicial submesh $\mathcal{T}_h$ such that*

(i) Shape-regularity. *There exists a real $\varrho_1 > 0$ independent of h such that, for all $h \in \mathcal{H}$ and all simplex $T \in \mathcal{T}_h$ of diameter h_T and inradius r_T, there holds $\varrho_1 h_T \leqslant r_T$;*

(ii) Contact-regularity. *There exists a real $\varrho_2 > 0$ independent of h such that, for all $h \in \mathcal{H}$, all $K \in \mathcal{K}_h$, and all $T \in \mathcal{T}_K := \{T \in \mathcal{T}_h \mid T \subset K\}$, there holds $\varrho_2 h_K \leqslant h_T$.*

2.2 Admissible mesh sequences

The discrete space introduced in this work requires to identify a set of points which play a pivotal role in the construction.

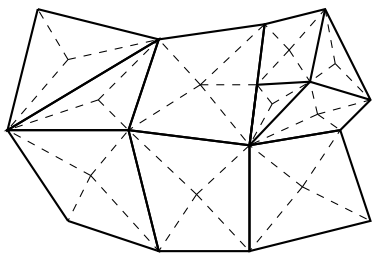

Figure 1: Mesh $\mathcal{K}_h$ (solid lines) and pyramidal submesh $\mathcal{P}_h$ (dashed lines)

Definition 2 (Cell centers)**.** *The mesh sequence $\mathcal{K}_\mathcal{H}$ admits a set of cell centers if, for all $h \in \mathcal{H}$ and all $K \in \mathcal{K}_h$, there exists a point $\boldsymbol{x}_K$ such that K is star-shaped with respect to $\boldsymbol{x}_K$ (the* cell center*) and, for all $F \in \mathcal{F}_K$, there holds,*

$$d_{K,F} \geqslant \varrho_3 h_K, \tag{1}$$

where $d_{K,F}$ denotes the orthogonal distance between $\boldsymbol{x}_K$ and F and $\varrho_3 > 0$ is independent of h.

Let $\mathcal{K}_\mathcal{H}$ admit a set of cell centers. We define for all $h \in \mathcal{H}$ the pyramidal submesh

$$\mathcal{P}_h = \{K_F\}_{K \in \mathcal{K}_h,\, F \in \mathcal{F}_K},$$

where, for all $K \in \mathcal{K}_h$ and all $F \in \mathcal{F}_K$, K_F denotes the open pyramid of apex $\boldsymbol{x}_K$ and base F. An example of mesh $\mathcal{K}_h$ and associated pyramidal submesh $\mathcal{P}_h$ is provided in Figure 1. Each element of $\mathcal{P}_h$ is associated to a unique element $K \in \mathcal{K}_h$ and a unique face $F \in \mathcal{F}_K$. When this link is irrelevant, the generic element of $\mathcal{P}_h$ is noted P instead of K_F. The pyramids $\{K_F\}_{K \in \mathcal{K}_h,\, F \in \mathcal{F}_K}$ are nondegenerated owing to assumption (1). In the two-dimensional case, $\mathcal{P}_h$ is matching and simplicial while, in higher dimension, it is in general not simplicial. Owing to the planarity of faces, there holds for all $K \in \mathcal{K}_h$ and all $F \in \mathcal{F}_K$,

$$|K_F| = \frac{|F|\, d_{K,F}}{d}. \tag{2}$$

The set of faces of $\mathcal{P}_h$ (including the mesh faces in $\mathcal{F}_{\mathcal{K}_h}$ as well as the lateral faces of the pyramids) is denoted by $\mathcal{F}_{\mathcal{P}_h}$ and we let $\mathcal{F}^{\mathrm{i}}_{\mathcal{P}_h} := \mathcal{F}_{\mathcal{P}_h} \backslash \mathcal{F}^{\mathrm{b}}_{\mathcal{K}_h}$ and $\mathcal{F}^{\mathrm{b}}_{\mathcal{P}_h} := \mathcal{F}^{\mathrm{b}}_{\mathcal{K}_h}$. Additionally, for all $P \in \mathcal{P}_h$, we introduce the set $\mathcal{F}_P := \{F \in \mathcal{F}_{\mathcal{P}_h} \mid F \subset \partial P\}$.

Lemma 3 (Shape- and contact-regularity of the pyramidal submesh)**.** *Let $\mathcal{K}_\mathcal{H}$ admit a set of cell centers. Then, if $\mathcal{K}_\mathcal{H}$ is shape- and contact-regular, the same holds for $\mathcal{P}_\mathcal{H}$.*

Proof. Let $h \in \mathcal{H}$. By assumption, $\mathcal{K}_h$ admits a matching simplicial submesh $\mathcal{T}_h$. A matching simplicial submesh $\mathfrak{T}_h$ of the pyramidal submesh $\mathcal{P}_h$ can be constructed as follows: For all $K \in \mathcal{K}_h$ and all $F \in \mathcal{F}_K$ (i) a $(d-1)$-simplicial mesh $\mathfrak{S}_F$ of F is obtained taking the trace of $\mathcal{T}_h$ on F; (ii) a d-simplicial mesh $\mathfrak{T}_{K_F}$ of the pyramid K_F is then obtained connecting the (hyperplanar) elements in $\mathfrak{S}_F$ to the cell center. A matching simplicial submesh of $\mathcal{P}_h$ is obtained by setting

$$\mathfrak{T}_h := \bigcup_{K \in \mathcal{K}_h,\, F \in \mathcal{F}_K} \mathfrak{T}_{K_F}.$$

(i) *Shape-regularity.* We prove that there exists a real $\varrho_1' > 0$ independent of h such that $\varrho_1' h_T \leqslant r_T$ for all $T \in \mathfrak{T}_h$. Let $K_F \in \mathcal{P}_h$ and $T \in \mathfrak{T}_{K_F}$ be given. Denoting by r_T the inradius of T, letting $\mathcal{A}_T := |\partial T|$ and $\sigma := \partial T \cap F$, there holds $d\,|T| = r_T \mathcal{A}_T = |\sigma|\, d_{K,F}$, hence

$$r_T = \frac{|\sigma|\, d_{K,F}}{\mathcal{A}_T}. \tag{3}$$

Since the $(d-1)$-dimensional measure of each face of T is bounded by h_K^{d-1} and T has $(d+1)$ faces, there holds $\mathcal{A}_T \leqslant (d+1)h_K^{d-1}$. Let now $S \in \mathcal{T}_h$ be the unique simplex such that $\partial S \cap F = \sigma$ and $S \subset K$. Denoting by r_σ the inradius of σ, and observing that $r_\sigma \geqslant r_S$ by a simple argument based on the Pythagorean theorem, it is inferred $|\sigma| \geqslant |\mathfrak{B}_{d-1}|\, r_\sigma^{d-1} \geqslant |\mathfrak{B}_{d-1}|\, r_S^{d-1} \geqslant |\mathfrak{B}_{d-1}|\,(\varrho_1\varrho_2)^{d-1} h_K^{d-1}$ owing to the shape- and contact-regularity of $\mathcal{K}_h$ ($\mathfrak{B}_{d-1}$ denotes here the $(d-1)$-dimensional unit ball). Plugging these inequalities into (3), it is inferred

$$r_T \geqslant \frac{|\mathfrak{B}_{d-1}|\,(\varrho_1\varrho_2)^{d-1}}{d+1} d_{K,F} \geqslant \varrho_3 \frac{|\mathfrak{B}_{d-1}|\,(\varrho_1\varrho_2)^{d-1}}{d+1} h_T,$$

and the conclusion follows with $\varrho_1' = \varrho_3\,|\mathfrak{B}_{d-1}|\,(\varrho_1\varrho_2)^{d-1}/(d+1)$.
(ii) *Contact-regularity.* We prove that there exists a real $\varrho_2' > 0$ independent of h such that, for all $K_F \in \mathcal{P}_h$ and all $T \in \mathfrak{T}_{K_F}$, $\varrho_2' h_{K_F} \leqslant h_T$. To this end, we invoke (1) to infer, for all $K_F \in \mathcal{P}_h$ and all $T \in \mathfrak{T}_{K_F}$, $h_T \geqslant d_{K,F} \geqslant \varrho_3 h_K \geqslant \varrho_3 h_{K_F}$, where h_{K_F} denotes the diameter of K_F. The conclusion follows with $\varrho_2' = \varrho_3$. □

We close this section with the following definition.

Definition 4 (Admissible mesh sequence)**.** *The mesh sequence $\mathcal{K}_\mathcal{H}$ is* admissible *if it is shape- and contact-regular and it admits a set of cell centers. For an admissible mesh sequence, the reals ϱ_1, ϱ_2, and ϱ_3, are collectively referred to as* mesh regularity parameters.

2.3 Broken function spaces and polynomial approximation

For $\mathcal{S}_h \in \{\mathcal{K}_h, \mathcal{P}_h\}$ and an integer $k \geqslant 0$, we introduce the broken polynomial space

$$\mathbb{P}_d^k(\mathcal{S}_h) := \{v \in L^2(\Omega) \mid \forall S \in \mathcal{S}_h,\ v_{|S} \in \mathbb{P}_d^k(S)\}, \tag{4}$$

where $\mathbb{P}_d^k$ denotes the space of polynomial functions of total degree at most k. Broken polynomial spaces are a special instance of broken Sobolev spaces: For an integer $l \geqslant 1$,

$$H^l(\mathcal{S}_h) := \{v \in L^2(\Omega) \mid \forall S \in \mathcal{S}_h,\ v_{|S} \in H^l(S)\}.$$

We define the broken gradient denoted by $\boldsymbol{\nabla}_h$ and acting on functions $v \in H^1(\mathcal{S}_h)$ such that $(\boldsymbol{\nabla}_h v)_{|S} := \boldsymbol{\nabla}(v_{|S})$, for all $S \in \mathcal{S}_h$. We also define the broken divergence of a vector-valued field $\boldsymbol{v} \in H^1(\mathcal{S}_h)^d$ denoted by $\boldsymbol{\nabla}_h \cdot \boldsymbol{v}$, and the broken symmetric gradient $\underline{\underline{\varepsilon_h}}(\boldsymbol{v})$ respectively as the trace and as the symmetric part of the broken tensor-gradient $\boldsymbol{\nabla}_h \boldsymbol{v}$. The shape- and contact-regularity of the mesh sequences $\mathcal{K}_\mathcal{H}$ and $\mathcal{P}_\mathcal{H}$ are instrumental to prove the following result, see [17, Lemmata 1.46 and 1.49].

Lemma 5 (Trace inequalities)**.** *Let $\mathcal{K}_\mathcal{H}$ be an admissible mesh sequence,and denote by $\mathcal{P}_\mathcal{H}$ the corresponding sequence of pyramidal submeshes. Then, there exist two reals C_{tr} and $C_{\mathrm{tr,c}}$ independent of h such that, for all $h \in \mathcal{H}$ with $\mathcal{S}_h \in \{\mathcal{K}_h, \mathcal{P}_h\}$,*

$$\forall v_h \in \mathbb{P}_d^k(\mathcal{P}_h),\ \forall P \in \mathcal{P}_h,\ \forall F \in \mathcal{F}_P, \qquad \|v_h\|_{L^2(F)} \leqslant C_{\mathrm{tr}} h_F^{-1/2} \|v_h\|_{L^2(P)}, \tag{5}$$

$$\forall v \in H^1(\mathcal{S}_h),\ \forall S \in \mathcal{S}_h,\ \forall F \in \mathcal{F}_S, \qquad \|v\|_{L^2(F)} \leqslant C_{\mathrm{tr,c}} \Big(h_S^{-1} \|v\|_{L^2(S)}^2 + h_S |v|_{H^1(S)}^2 \Big)^{1/2}. \tag{6}$$

For every interface $F \in \mathcal{F}_{\mathcal{S}_h}^{\mathrm{i}}$, $\mathcal{S}_h \in \{\mathcal{K}_h, \mathcal{P}_h\}$, we introduce an arbitrary but fixed ordering of the elements S_1 and S_2 such that $F \subset \partial S_1 \cap \partial S_2$ and let $\boldsymbol{n}_F := \boldsymbol{n}_{S_1,F} = -\boldsymbol{n}_{S_2,F}$, where $\boldsymbol{n}_{S_i,F}$, $i \in \{1,2\}$, denotes the unit normal to F pointing out of S_i. The orientation of the normal remains coherent when $F \in \mathcal{F}_{\mathcal{K}_h}^{\mathrm{i}}$ is regarded as an element of $\mathcal{F}_{\mathcal{P}_h}^{\mathrm{i}}$. For all $S \in \mathcal{S}_h$, we

also introduce the symbol $\boldsymbol{n}_S$ to denote the vector-valued field such that $\boldsymbol{n}_{S|F} = \boldsymbol{n}_{S,F}$ for all $F \in \mathcal{F}_S$. On boundary faces $F \in \mathcal{F}^{\mathrm{b}}_{\mathcal{P}_h}$, $\boldsymbol{n}_F$ denotes the unit normal pointing out of Ω.

We next introduce jump and average trace operators that are widely used in the context of nonconforming finite element methods. For a face $F \in \mathcal{F}^{\mathrm{i}}_{\mathcal{P}_h}$ with $F \subset \partial P_1 \cap \partial P_2$ and a scalar-valued function v admitting a possibly two-valued trace on F we set,

$$[\![v]\!]_F := v_{|P_1} - v_{|P_2}, \qquad \{v\}_F := \frac{1}{2}\left(v_{|P_1} + v_{|P_2}\right).$$

If $F \in \mathcal{F}^{\mathrm{b}}_{\mathcal{P}_h}$ with $F = \partial P \cap \partial\Omega$, we conventionally set $[\![v]\!]_F = \{v\}_F := v_{|P}$. When applied to vector-valued functions, both the jump and average operators act component-wise. Whenever no confusion can arise, we omit the subscript F and simply write $[\![v]\!]$, $\{v\}$.

We close this section by considering polynomial approximation on admissible mesh sequences. It has been proved in [17, Lemma 1.40] that, for a shape- and contact-regular mesh sequence, the number of simplices from the submesh $\mathcal{T}_h$ contained in each element $K \in \mathcal{K}_h$ is bounded uniformly in h. This, together with the results of Dupont and Scott [23], yields the following.

Lemma 6 (Optimal polynomial approximation)**.** *Let $\mathcal{K}_{\mathcal{H}}$ denote a shape- and contact-regular mesh sequence. Then, for all $h \in \mathcal{H}$, all $K \in \mathcal{K}_h$, all polynomial degree $k \geqslant 0$, all $s \in \{0, \ldots, k+1\}$ and all $v \in H^s(K)$, there holds with Π^k_h denoting the L^2-orthogonal projector onto $\mathbb{P}^k_d(\mathcal{K}_h)$,*

$$|v - \Pi^k_h v|_{H^m(K)} \leqslant C_{\mathrm{app}} h_K^{s-m} |v|_{H^s(K)} \qquad \forall\, m \in \{0, \ldots, s\}, \tag{7}$$

where C_{app} is independent of both K and h.

We also note the following result, which is an immediate consequence of the trace inequality (6) with $\mathcal{S}_h = \mathcal{K}_h$ and of the approximation properties of the L^2-orthogonal projector.

Proposition 7 (Approximation on mesh faces)**.** *For an admissible mesh sequence $\mathcal{K}_{\mathcal{H}}$ there holds for all $h \in \mathcal{H}$, all $K \in \mathcal{K}_h$, all $F \in \mathcal{F}_K$, all polynomial degree $k \geqslant 0$, all $s \in \{0, \ldots, k+1\}$, and all $v \in H^s(K)$,*

$$\|v - \Pi^k_h v\|_{L^2(F)} \leqslant C h_K^{s-1/2} |v|_{H^s(K)},$$

where $C = C_{\mathrm{tr,c}} C_{\mathrm{app}}$ with $C_{\mathrm{tr,c}}$ defined as in (6) and C_{app} as in (7).

3 Mimicking the properties of the lowest-order Crouzeix–Raviart space on general meshes

In this section we present a piecewise affine functional space obtained in the spirit of [16] that extends the properties (CR1) and (CR2) of the Crouzeix–Raviart space [15] to general polygonal or polyhedral meshes.

3.1 Construction

In the spirit of ccG methods, we proceed in three steps by prescribing (i) the vector space of degrees of freedom $\mathbb{V}_h$; (ii) a gradient reconstruction $\mathfrak{G}_h$, piecewise constant on $\mathcal{P}_h$; (iii) a piecewise affine reconstruction $\mathfrak{R}_h$ on $\mathcal{P}_h$, based on the gradient $\mathfrak{G}_h$. As for HFV methods [25], the vector space of DOFs contains cell and face unknowns and is defined by

$$\mathbb{V}_h := \left\{ \mathbb{v}_h = \left((v_K \in \mathbb{R})_{K \in \mathcal{K}_h}, (v_F \in \mathbb{R})_{F \in \mathcal{F}_{\mathcal{K}_h}} \right) \in \mathbb{R}^{\mathcal{K}_h} \times \mathbb{R}^{\mathcal{F}_{\mathcal{K}_h}} \right\}.$$

The gradient operator generalizes the one of [25], and is composed of a consistent contribution piecewise constant on the primal mesh $\mathcal{K}_h$ plus a subgrid correction piecewise constant on the pyramidal submesh $\mathcal{P}_h$. More precisely, $\mathfrak{G}_h : \mathbb{V}_h \to \mathbb{P}_d^0(\mathcal{P}_h)^d$ realizes the mapping $\mathbb{v}_h \mapsto \mathfrak{G}_h(\mathbb{v}_h)$ with

$$\mathfrak{G}_h(\mathbb{v}_h)_{|K_F} = \boldsymbol{G}_{K_F}(\mathbb{v}_h) := \boldsymbol{G}_K(\mathbb{v}_h) + \boldsymbol{R}_{K_F}(\mathbb{v}_h), \qquad \forall K \in \mathcal{K}_h,\, F \in \mathcal{F}_K, \tag{8}$$

where, letting $\overline{\boldsymbol{x}}_F := \langle \boldsymbol{x} \rangle_F$ (for a function φ integrable on F, we define $\langle \varphi \rangle_F := \int_F \varphi / |F|$),

$$\boldsymbol{G}_K(\mathbb{v}_h) := \frac{1}{|K|} \sum_{F \in \mathcal{F}_K} |F|\, v_F \boldsymbol{n}_{K,F}, \quad \boldsymbol{R}_{K_F}(\mathbb{v}_h) := \frac{\eta}{d_{K,F}} \left(v_F - v_K - \boldsymbol{G}_K(\mathbb{v}_h) \cdot (\overline{\boldsymbol{x}}_F - \boldsymbol{x}_K) \right) \boldsymbol{n}_{K,F}, \tag{9}$$

and $\eta > 0$ is a user-dependent parameter. With a slight abuse in notation, the symbols $\boldsymbol{G}_{K_F}(\mathbb{v}_h)$, $\boldsymbol{G}_K(\mathbb{v}_h)$, and $\boldsymbol{R}_{K_F}(\mathbb{v}_h)$ will also be used to denote the corresponding constant fields on K_F, K, and K_F, respectively. The reconstruction operator $\mathfrak{R}_h : \mathbb{V}_h \to \mathbb{P}_d^1(\mathcal{P}_h)$ realizes the mapping $\mathbb{v}_h \mapsto \mathfrak{R}_h(\mathbb{v}_h)$ with

$$\mathfrak{R}_h(\mathbb{v}_h)_{|K_F}(\boldsymbol{x}) = v_F + \mathfrak{G}_h(\mathbb{v}_h)_{|K_F} \cdot (\boldsymbol{x} - \overline{\boldsymbol{x}}_F), \qquad \forall K_F \in \mathcal{P}_h,\, \forall \boldsymbol{x} \in K_F. \tag{10}$$

By construction, there holds $\boldsymbol{\nabla}_h \mathfrak{R}_h = \mathfrak{G}_h$. We emphasize that, in view of Lemma 8 below, the affine reconstruction in K_F is obtained by perturbing the face unknown v_F, unlike [16], where the cell unknown v_K is used instead. We are now ready to introduce the discrete space

$$\mathfrak{CR}(\mathcal{K}_h) := \mathfrak{R}_h(\mathbb{V}_h). \tag{11}$$

3.2 Continuity of mean values at interfaces

In this section we prove that the choice $\eta = d$ in (9) yields the continuity of the mean values (or, equivalently, the barycentric values) of discrete functions across all the interfaces in $\mathcal{F}^{\mathrm{i}}_{\mathcal{P}_h}$ (including lateral pyramidal faces). This is in contrast with the choice $\eta = d^{1/2}$ advocated in [25] to recover the two-point finite volume scheme on superadmissible meshes.

Lemma 8 (Continuity of mean values at interfaces)**.** *Let $\mathcal{K}_h$ belong to an admissible mesh sequence and, if $\mathcal{K}_h$ is not matching simplicial, assume $\eta = d$ in* (9)*. Then, there holds for all $v_h \in \mathfrak{CR}(\mathcal{K}_h)$,*

$$\forall F \in \mathcal{F}^{\mathrm{i}}_{\mathcal{P}_h}, \qquad \langle [\![v_h]\!] \rangle_F = 0.$$

Proof. Let $F \in \mathcal{F}^{\mathrm{i}}_{\mathcal{P}_h}$, $\mathbb{v}_h \in \mathbb{V}_h$, and set $v_h := \mathfrak{R}_h(\mathbb{v}_h) \in \mathfrak{CR}(\mathcal{K}_h)$. We distinguish two cases. (i) If $F \in \mathcal{F}^{\mathrm{i}}_{\mathcal{K}_h}$ is a face of the primal mesh $\mathcal{K}_h$, the fact that $\langle [\![v_h]\!] \rangle_F = 0$ is an immediate consequence of choosing v_F as a starting point in (10). (ii) If $F \in \mathcal{F}^{\mathrm{i}}_{\mathcal{P}_h} \backslash \mathcal{F}^{\mathrm{i}}_{\mathcal{K}_h}$ is a lateral pyramidal face, there exist a unique element $K \in \mathcal{K}_h$ and two faces F_1, $F_2 \in \mathcal{F}_K$ such that $F \subset \partial K_{F_1} \cap \partial K_{F_2}$ (cf. Figure 2a). There holds for $i \in \{1, 2\}$ (cf. Figure 2b),

$$(\overline{\boldsymbol{x}}_F - \overline{\boldsymbol{x}}_{F_i}) \cdot \boldsymbol{n}_{K,F_i} = (\overline{\boldsymbol{x}}_F - \boldsymbol{x}_K) \cdot \boldsymbol{n}_{K,F_i} + (\boldsymbol{x}_K - \overline{\boldsymbol{x}}_{F_i}) \cdot \boldsymbol{n}_{K,F_i} = \left(\frac{d-1}{d} - 1 \right) d_{K,F_i} = -\frac{d_{K,F_i}}{d},$$

where we have used the fact that $\overline{\boldsymbol{x}}_F$ is the barycenter of the $(d-1)$-simplex F to treat the term $(\overline{\boldsymbol{x}}_F - \boldsymbol{x}_K) \cdot \boldsymbol{n}_{K,F_i}$. Using the above result together with (9) it is inferred for $i \in \{1, 2\}$,

$$\alpha_i := \boldsymbol{R}_{K_{F_i}}(\mathbb{v}_h) \cdot (\overline{\boldsymbol{x}}_F - \overline{\boldsymbol{x}}_{F_i}) = -\frac{\eta}{d} \left(v_{F_i} - v_K - \boldsymbol{G}_K(\mathbb{v}_h) \cdot (\overline{\boldsymbol{x}}_{F_i} - \boldsymbol{x}_K) \right).$$

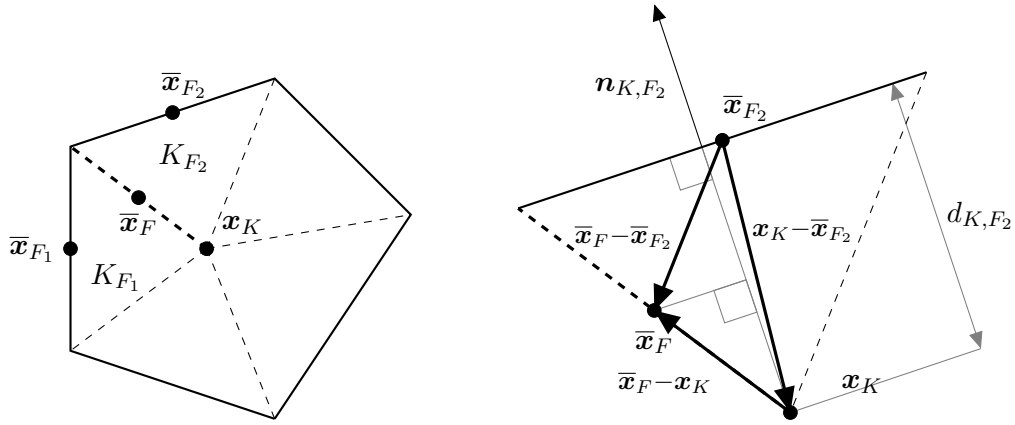

(a) Element K (solid line), elementary pyramidal submesh (dashed line), and lateral pyramidal face F shared by the pyramids K_{F_1} and K_{F_2} (thick dashed line)

(b) Zoom on the pyramid K_{F_2}

Figure 2: Notation for the proof of Lemma 8

Using the definition of the jump operator and substituting the expression (10) for the barycentric values $v_{h|K_{F_i}}(\overline{\boldsymbol{x}}_F)$, $i \in \{1,2\}$, we obtain

$$\begin{aligned}\langle [\![v_h]\!] \rangle_F &= v_{h|K_{F_1}}(\overline{\boldsymbol{x}}_F) - v_{h|K_{F_2}}(\overline{\boldsymbol{x}}_F) = v_{F_1} - v_{F_2} - \boldsymbol{G}_K(\mathbb{v}_h)\cdot(\overline{\boldsymbol{x}}_{F_1} - \overline{\boldsymbol{x}}_{F_2}) + \alpha_1 - \alpha_2 \\ &= \left(1 - \frac{\eta}{d}\right)\left(v_{F_1} - v_{F_2} - \boldsymbol{G}_K(\mathbb{v}_h)\cdot(\overline{\boldsymbol{x}}_{F_1} - \overline{\boldsymbol{x}}_{F_2})\right).\end{aligned} \tag{12}$$

If $\mathcal{K}_h$ is a matching simplicial mesh, $\boldsymbol{G}_K(\mathbb{v}_h)$ coincides by definition with the standard Crouzeix–Raviart gradient (cf. also Proposition 9), hence the second factor in (12) vanishes, otherwise the assumption $\eta = d$ is needed to infer $\langle [\![v_h]\!] \rangle_F = 0$, thereby concluding the proof. □

The following result establishes a link with the classical Crouzeix–Raviart space $\mathbb{CR}(\mathcal{K}_h)$.

Proposition 9 (The matching simplicial case)**.** *Assume that $\mathcal{K}_h$ is a matching simplicial mesh. Then, for all $\eta > 0$ in* (9) *there holds*

$$\mathbb{CR}(\mathcal{K}_h) \subset \mathfrak{CR}(\mathcal{K}_h). \tag{13}$$

Proof. Let $v_h \in \mathbb{CR}(\mathcal{K}_h)$ and set $\mathbb{v}_h := ((v_h(\boldsymbol{x}_K))_{K\in\mathcal{K}_h}, (v_h(\overline{\boldsymbol{x}}_F))_{F\in\mathcal{F}_{\mathcal{K}_h}})$. By definition there holds (cf. (9)) $\boldsymbol{G}_K(\mathbb{v}_h) = (\boldsymbol{\nabla}_h v_h)_{|K}$ for all $K \in \mathcal{K}_h$. Using the linearity of v_h inside each element it is inferred $\boldsymbol{R}_{K_F}(\mathbb{v}_h) = \boldsymbol{0}$, hence $\boldsymbol{G}_{K_F}(\mathbb{v}_h) = \boldsymbol{G}_K(\mathbb{v}_h) = (\boldsymbol{\nabla}_h v_h)_{|K}$ for all $F \in \mathcal{F}_K$. As a consequence, we conclude that $v_h = \mathfrak{R}_h(\mathbb{v}_h) \in \mathfrak{CR}(\mathcal{K}_h)$. □

3.3 Approximation

In this section we introduce a suitable interpolator on $\mathfrak{CR}(\mathcal{K}_h)$ and study its approximation properties. Let $\mathcal{I}_h^{\mathfrak{CR}} : H^1(\Omega) \to \mathfrak{CR}(\mathcal{K}_h)$ be such that, for all $v \in H^1(\Omega)$, $\mathcal{I}_h^{\mathfrak{CR}}(v) = \mathfrak{R}_h(\mathbb{v}_h)$ with

$$\mathbb{V}_h \ni \mathbb{v}_h = ((\Pi_h^1 v(\boldsymbol{x}_K))_{K\in\mathcal{K}_h}, (\langle v \rangle_F)_{F\in\mathcal{F}_{\mathcal{K}_h}}). \tag{14}$$

When applied to vector-valued fields, $\mathcal{I}_h^{\mathfrak{CR}}$ acts component-wise.

Lemma 10 (Approximation in $\mathfrak{CR}(\mathcal{K}_h)$)**.** *For all $\eta > 0$ in (9) and all $v \in H^1(\Omega)$ there holds with $v_h := \mathcal{I}_h^{\mathfrak{CR}}(v) \in \mathfrak{CR}(\mathcal{K}_h)$,*

$$\Pi_h^0(\boldsymbol{\nabla}_h v_h) = \Pi_h^0(\boldsymbol{\nabla} v), \tag{15}$$

where Π_h^0 denotes the L^2-orthogonal projector on $\mathbb{P}_d^0(\mathcal{K}_h)^d$. Moreover, there exists a real $C > 0$ independent of the meshsize such that, for all $h \in \mathcal{H}$, all $K \in \mathcal{K}_h$, all $v \in H^1(\Omega) \cap H^{l+1}(\mathcal{K}_h)$, $l \in \{0, 1\}$, there holds with $v_h := \mathcal{I}_h^{\mathfrak{CR}}(v)$

$$\|v - v_h\|_{L^2(K)} + h_K \|\boldsymbol{\nabla} v - \boldsymbol{\nabla}_h v_h\|_{L^2(K)^d} \leqslant C h_K^{l+1} |v|_{H^{l+1}(K)}. \tag{16}$$

Proof. To avoid naming generic constants, we use the notation $a \lesssim b$ for the inequality $a \leqslant Cb$ with $C > 0$ independent of the meshsize.
(i) *Equality* (15). For a given $v \in H^1(\Omega)$, let $\mathbb{v}_h$ be defined as in (14). We start by noting the following orthogonality relation (cf. [25, eq. (27)]) valid for all $\mathbb{w}_h \in \mathbb{V}_h$ and all $K \in \mathcal{K}_h$:

$$\sum_{F \in \mathcal{F}_K} |K_F| \, \boldsymbol{R}_{K_F}(\mathbb{w}_h) = \mathbf{0}. \tag{17}$$

As a consequence, for all $K \in \mathcal{K}_h$ there holds,

$$\Pi_h^0(\boldsymbol{\nabla}_h v_h)_{|K} = \boldsymbol{G}_K(\mathbb{v}_h) = \frac{1}{|K|} \sum_{F \in \mathcal{F}_K} |F| \langle v \rangle_F \boldsymbol{n}_{K,F} = \frac{1}{|K|} \int_{\partial K} v \boldsymbol{n}_K = \Pi_h^0(\boldsymbol{\nabla} v)_{|K},$$

where we have used the planarity of faces and Green's formula. Relation (15) follows.
(ii) *Inequality* (16). Let $v \in H^1(\Omega) \cap H^{l+1}(\mathcal{K}_h)$ and define $\mathbb{v}_h$ as in (14). We first estimate $\|\boldsymbol{\nabla} v - \boldsymbol{\nabla}_h v_h\|_{L^2(K)^d}$, $K \in \mathcal{K}_h$. Using (8), the previous point, and the triangular inequality we infer

$$\|\boldsymbol{\nabla} v - \boldsymbol{\nabla}_h v_h\|_{L^2(K)^d} \leqslant \|\boldsymbol{\nabla} v - \Pi_h^0(\boldsymbol{\nabla} v)\|_{L^2(K)^d} + \left(\sum_{F \in \mathcal{F}_K} |K_F| \, |\boldsymbol{R}_{K_F}(\mathbb{v}_h)|^2 \right)^{\frac{1}{2}} := \mathfrak{T}_1 + \mathfrak{T}_2.$$

Using the approximation properties of the L^2-orthogonal projector it is readily inferred $\mathfrak{T}_1 \lesssim h_K^l |v|_{H^{l+1}(K)}$. To estimate the second term, we preliminarily observe that there holds for all $F \in \mathcal{F}_K$ with $w_h := \Pi_h^1 v$ (Π_h^1 denotes here the L^2-orthogonal projector on $\mathbb{P}_d^1(\mathcal{K}_h)$),

$$\boldsymbol{R}_{K_F}(\mathbb{v}_h) = \frac{\eta}{d_{K,F}} \left(\langle v \rangle_F - w_h(\boldsymbol{x}_K) - \boldsymbol{G}_K(\mathbb{v}_h) \cdot (\overline{\boldsymbol{x}}_F - \boldsymbol{x}_K) \right) \boldsymbol{n}_{K,F} = \frac{\eta}{d_{K,F}} \left(\alpha_{K,F} + \beta_{K,F} \right) \boldsymbol{n}_{K,F}, \tag{18}$$

where $\alpha_{K,F} := \langle v \rangle_F - \langle w_{h|K} \rangle_F$, $\beta_{K,F} := \left(\boldsymbol{\nabla} w_{h|K} - \boldsymbol{G}_K(\mathbb{v}_h) \right) \cdot (\overline{\boldsymbol{x}}_F - \boldsymbol{x}_K)$, and, since $w_{h|K}$ is affine in K, $w_h(\boldsymbol{x}_K) = \langle w_{h|K} \rangle_F - \boldsymbol{\nabla} w_{h|K} \cdot (\overline{\boldsymbol{x}}_F - \boldsymbol{x}_K)$. There follows from equation (18)

$$\mathfrak{T}_2^2 \lesssim \sum_{F \in \mathcal{F}_K} \frac{|K_F|}{d_{K,F}^2} |\alpha_{K,F}|^2 + \sum_{F \in \mathcal{F}_K} \frac{|K_F|}{d_{K,F}^2} |\beta_{K,F}|^2 := \mathfrak{T}_{2,1} + \mathfrak{T}_{2,2}.$$

Using (2), the Cauchy–Schwarz inequality, the mesh regularity assumption (1), the fact that $\mathrm{card}(\mathcal{F}_K)$ is bounded uniformly in h (cf. [17, Lemma 1.41]), and Proposition 7 it is inferred,

$$\mathfrak{T}_{2,1} = \frac{1}{d} \sum_{F \in \mathcal{F}_K} \frac{1}{d_{K,F} \, |F|} \left(\int_F v - w_h \right)^2 \leqslant \frac{1}{d \varrho_3} \sum_{F \in \mathcal{F}_K} \frac{1}{h_K} \|v - w_h\|_{L^2(F)}^2 \lesssim h_K^{2l} |v|_{H^{l+1}(K)}^2.$$

On the other hand, since $|\overline{\boldsymbol{x}}_F - \boldsymbol{x}_K| \leqslant h_K$ and both $\boldsymbol{\nabla} w_{h|K}$ and $\boldsymbol{G}_K(\mathbb{v}_h)$ are constant on K, there holds

$$\mathfrak{T}_{2,2} \leqslant \sum_{F \in \mathcal{F}_K} |K_F| \frac{h_K^2}{d_{K,F}^2} |\boldsymbol{\nabla} w_{h|K} - \boldsymbol{G}_K(\mathbb{v}_h)|^2 \leqslant \frac{1}{\varrho_3^2} \|\boldsymbol{\nabla} w_{h|K} - \Pi_h^0(\boldsymbol{\nabla} v)\|_{L^2(K)^d}^2 \lesssim h_K^{2l} |v|_{H^{l+1}(K)}^2,$$

where we have used the mesh regularity assumption (1) together with (15), and concluded using the approximation properties of the L^2-orthogonal projector. Gathering up the bounds on $\mathfrak{T}_1$ and $\mathfrak{T}_2$ it is inferred

$$\|\boldsymbol{\nabla} v - \boldsymbol{\nabla}_h v_h\|_{L^2(K)^d} \lesssim h_K^l |v|_{H^{l+1}(K)}. \tag{19}$$

To complete the proof of inequality (16) it only remains to estimate $\|v - v_h\|_{L^2(K)}$. To this end, letting again $w_h := \Pi_h^1 v$, we apply the triangular inequality to infer

$$\|v - v_h\|_{L^2(K)} \leqslant \|v - w_h\|_{L^2(K)} + \|w_h - v_h\|_{L^2(K)} := \mathfrak{T}_1 + \mathfrak{T}_2.$$

The approximation properties of the L^2-orthogonal projector readily yield $\mathfrak{T}_1 \lesssim h_K^{l+1}|v|_{H^{l+1}(K)}$. For the second term, we notice that for all $F \in \mathcal{F}_K$ and all $\boldsymbol{x} \in K_F$, the linearity of both $w_{h|K}$ and $v_{h|K_F}$ yields

$$w_{h|K}(\boldsymbol{x}) = \langle w_{h|K} \rangle_F + \boldsymbol{\nabla} w_{h|K} \cdot (\boldsymbol{x} - \overline{\boldsymbol{x}}_F), \quad v_{h|K_F}(\boldsymbol{x}) = \langle v \rangle_F + \boldsymbol{\nabla} v_{h|K_F} \cdot (\boldsymbol{x} - \overline{\boldsymbol{x}}_F).$$

As a consequence,

$$\|w_h - v_h\|^2_{L^2(K_F)} \lesssim \int_{K_F} (\langle w_{h|K} - v \rangle_F)^2 + \int_{K_F} \left[(\boldsymbol{\nabla} w_{h|K} - \boldsymbol{\nabla} v_{h|K_F}) \cdot (\boldsymbol{x} - \overline{\boldsymbol{x}}_F) \right]^2 := \mathfrak{T}_{2,1} + \mathfrak{T}_{2,2}.$$

Using (2), the Cauchy–Schwarz inequality, and Proposition 7 it is inferred

$$\mathfrak{T}_{2,1} = \frac{|F|\, d_{K,F}}{d} (\langle w_{h|K} - v \rangle_F)^2 \leqslant \frac{d_{K,F}}{d} \|w_{h|K} - v\|^2_{L^2(F)} \lesssim h_K^{2(l+1)} |v|^2_{H^{l+1}(K)}.$$

Since $|\boldsymbol{x} - \overline{\boldsymbol{x}}_F| \leqslant h_K$ for all $\boldsymbol{x} \in K_F$ and both $\boldsymbol{\nabla} w_{h|K}$ and $\boldsymbol{\nabla} v_{h|K_F}$ are constant on K_F, the estimate (19) yields

$$\mathfrak{T}_{2,2} \leqslant h_K^2 \|\boldsymbol{\nabla} w_{h|K} - \boldsymbol{\nabla} v_{h|K_F}\|^2_{L^2(K_F)^d} \lesssim h_K^{2(l+1)} |v|^2_{H^{l+1}(K)}.$$

Summing over $F \in \mathcal{F}_K$, using the bounds for $\mathfrak{T}_{2,1}$ and $\mathfrak{T}_{2,2}$ together with the fact that $\mathrm{card}(\mathcal{F}_K)$ is bounded uniformly in h, it is inferred $\mathfrak{T}_2 \lesssim h_K^{l+1}|v|_{H^{l+1}(K)}$, thereby yielding $\|v - v_h\|_{L^2(K)} \lesssim h_K^{l+1}|v|_{H^{l+1}(K)}$, and therefore concluding the proof. □

Remark 11 (The matching simplicial case)**.** *When $\mathcal{K}_h$ is matching simplicial, the proof of Lemma 10 can be simplified exploiting the result of Proposition 9 to infer*

$$\inf_{v_h \in \mathfrak{CR}(\mathcal{K}_h)} \|v - v_h\|_{H^1(K)} \leqslant \inf_{v_h \in \mathbb{CR}(\mathcal{K}_h)} \|v - v_h\|_{H^1(K)},$$

and conclude using the approximation properties of the standard Crouzeix–Raviart space.

For all $\boldsymbol{w} \in \boldsymbol{H}(\mathrm{div}; \mathcal{K}_h) := \{\boldsymbol{v} \in L^2(\Omega)^d \mid \forall K \in \mathcal{K}_h, \boldsymbol{\nabla} \cdot (\boldsymbol{v}_{|K}) \in L^2(K)\}$ let

$$D_h(\boldsymbol{w}) := \Pi_h^0(\boldsymbol{\nabla}_h \cdot \boldsymbol{w}). \tag{20}$$

An immediate consequence of the first point in Lemma 10 is that the discrete vector space $\mathfrak{CR}(\mathcal{K}_h)^d$ possesses the following approximation property.

Corollary 12 (Divergence approximation)**.** *Let $\boldsymbol{v} \in H^1(\Omega)^d$ and $\boldsymbol{v}_h := \mathcal{I}_h^{\mathfrak{CR}}(\boldsymbol{v})$. There holds*

$$D_h(\boldsymbol{v}_h) = \Pi_h^0(\boldsymbol{\nabla} \cdot \boldsymbol{v}).$$

Moreover, there exists a real $C > 0$ independent of the meshsize such that, for all $h \in \mathcal{H}$, all $K \in \mathcal{K}_h$, and all $\boldsymbol{v} \in H^1(\Omega)^d \cap \boldsymbol{H}^1(\mathrm{div}; \mathcal{K}_h)$ with $\boldsymbol{H}^1(\mathrm{div}; \mathcal{K}_h) := \{\boldsymbol{v} \in \boldsymbol{H}(\mathrm{div}; \Omega) \mid \boldsymbol{\nabla}_h \cdot \boldsymbol{v} \in H^1(\mathcal{K}_h)\}$ and $\boldsymbol{v}_h := \mathcal{I}_h^{\mathfrak{CR}}(\boldsymbol{v})$,

$$\|\boldsymbol{\nabla} \cdot \boldsymbol{v} - D_h(\boldsymbol{v}_h)\|_{L^2(K)} + h_K |\boldsymbol{\nabla} \cdot \boldsymbol{v} - D_h(\boldsymbol{v}_h)|_{H^1(K)} \leqslant C h_K |\boldsymbol{\nabla} \cdot \boldsymbol{v}|_{H^1(K)}.$$

Thus, according to Corollary 12 and Lemma 10 (which gives an H^1-stability property), $\mathcal{I}_h^{\mathfrak{CR}}$ can play the role of a Fortin operator [10] for the Stokes problem; see the proof of Lemma 26.

4 Applications

In this section we present two applications where the properties of the discrete space (11) are instrumental in designing a suitable numerical approximation, namely linear elasticity for quasi-incompressible materials and the Stokes problem.

4.1 Discrete H_0^1-norm

For problems naturally set in $H_0^1(\Omega)$, boundary conditions can be accounted for in a strong manner by introducing the following subspace of $\mathfrak{CR}(\mathcal{K}_h)$:

$$\mathfrak{CR}_0(\mathcal{K}_h) := \mathfrak{R}_h(\mathbb{V}_{h,0}), \qquad \mathbb{V}_{h,0} = \{\mathbb{v}_h \in \mathbb{V}_h \mid v_F = 0, \forall F \in \mathcal{F}_{\mathcal{K}_h}^{\mathrm{b}}\}. \tag{21}$$

In the following proposition we show that the L^2-norm of the broken gradient is a norm on $\mathfrak{CR}_0(\mathcal{K}_h)$ by proving uniform discrete equivalence with the usual dG norm, cf. [17, Section 5.1]:

$$\|v_h\|_{\mathrm{dG}}^2 := \|\boldsymbol{\nabla}_h v_h\|_{L^2(\Omega)^d}^2 + |v_h|_{\mathrm{J}}^2, \qquad |v_h|_{\mathrm{J}}^2 := \sum_{F\in\mathcal{F}_{\mathcal{P}_h}} \frac{1}{h_F}\|[\![v_h]\!]\|_{L^2(F)}^2. \tag{22}$$

Proposition 13 (Discrete norm)**.** *Assume $\eta = d$ in (9). Then, there exists a real $C > 0$ independent of the meshsize such that, for all $v_h \in \mathfrak{CR}_0(\mathcal{K}_h)$,*

$$\|\boldsymbol{\nabla}_h v_h\|_{L^2(\Omega)^d} \leqslant \|v_h\|_{\mathrm{dG}} \leqslant C\|\boldsymbol{\nabla}_h v_h\|_{L^2(\Omega)^d}.$$

Proof. The notation $a \lesssim b$ stands for $a \leqslant Cb$ with $C > 0$ independent of the meshsize. Clearly, $\|\boldsymbol{\nabla}_h v_h\|_{L^2(\Omega)^d} \leqslant \|v_h\|_{\mathrm{dG}}$ for all $v_h \in \mathfrak{CR}_0(\mathcal{K}_h)$. To prove that $\|v_h\|_{\mathrm{dG}} \lesssim \|\boldsymbol{\nabla}_h v_h\|_{L^2(\Omega)^d}$ for all $v_h \in \mathfrak{CR}_0(\mathcal{K}_h)$, it suffices to show that $|v_h|_{\mathrm{J}} \lesssim \|\boldsymbol{\nabla}_h v_h\|_{L^2(\Omega)^d}$. Let $P \in \mathcal{P}_h$ and $F \in \mathcal{F}_P$. Owing to the linearity of v_h inside P there holds for all $\boldsymbol{x} \in P$, $v_{h|P}(\boldsymbol{x}) = \langle v_{h|P}\rangle_F + \boldsymbol{\nabla} v_{h|P} \cdot (\boldsymbol{x} - \overline{\boldsymbol{x}}_F)$. This together with Lemma 8 and the discrete trace inequality (5) yields

$$\|[\![v_h]\!]\|_{L^2(F)} = \|[\![v_h]\!] - \langle [\![v_h]\!]\rangle_F\|_{L^2(F)} \leqslant h_F\|[\![\boldsymbol{\nabla}_h v_h]\!]\|_{L^2(F)^d} \lesssim h_F^{1/2} \sum_{P\in\mathcal{P}_F} \|\boldsymbol{\nabla} v_{h|P}\|_{L^2(P)^d}, \tag{23}$$

where we have set $\mathcal{P}_F := \{P \in \mathcal{P}_h \mid F \subset \partial P\}$. Using (22) together with (23) and the Cauchy–Schwarz inequality it is inferred

$$|v_h|_{\mathrm{J}}^2 = \sum_{F\in\mathcal{F}_{\mathcal{P}_h}} \frac{1}{h_F}\|[\![v_h]\!] - \langle [\![v_h]\!]\rangle_F\|_{L^2(F)}^2 \lesssim \sum_{F\in\mathcal{F}_{\mathcal{P}_h}} \sum_{P\in\mathcal{P}_F} \|\boldsymbol{\nabla} v_{h|P}\|_{L^2(P)^d}^2 \lesssim \|\boldsymbol{\nabla}_h v_h\|_{L^2(\Omega)^d}^2, \tag{24}$$

where the last bound is a consequence of the fact that the maximum number of faces of a pyramid is bounded uniformly in h since $\mathcal{P}_h$ is shape- and contact-regular, cf. [17, Lemma 1.41]. □

4.2 Quasi-incompressible linear elasticity

We tackle here the question of the accurate approximation of the linear elasticity equations in the quasi-incompressible limit on general polygonal or polyhedral meshes. The main sources of inspiration are the classical works of Brenner and Sung [9], and Hansbo and Larson [28, 29].

4.2.1 Setting

We consider a homogeneous elastic material occupying the polygonal/polyhedral domain $\Omega \subset \mathbb{R}^d$, and whose mechanical properties are described by the real Lamé parameters λ and μ with $0 < \mu < +\infty$ and $0 < \lambda \leqslant +\infty$. The mechanical behavior of the material is governed by the linear elasticity equations,

$$\begin{aligned} -\boldsymbol{\nabla}\cdot\underline{\underline{\sigma}}(\boldsymbol{u}) &= \boldsymbol{f} \qquad \text{in } \Omega, \\ \boldsymbol{u} &= \boldsymbol{0} \qquad \text{on } \partial\Omega, \end{aligned} \tag{25}$$

where $\boldsymbol{u}$ denotes the vector-valued displacement field, $\boldsymbol{f} \in L^2(\Omega)^d$ the forcing term, and the Cauchy stress tensor is defined for all $\boldsymbol{v} \in H^1(\Omega)^d$ by Hooke's law,

$$\underline{\underline{\sigma}}(\boldsymbol{v}) := 2\mu\underline{\underline{\varepsilon}}(\boldsymbol{v}) + \lambda\boldsymbol{\nabla}\cdot\boldsymbol{v}\underline{\underline{I_d}}, \qquad \underline{\underline{\varepsilon}}(\boldsymbol{v}) := \frac{1}{2}(\boldsymbol{\nabla}\boldsymbol{v} + \boldsymbol{\nabla}\boldsymbol{v}^T).$$

Setting $\boldsymbol{U} := H^1_0(\Omega)^d$, the weak formulation of problem (25) reads: Find $\boldsymbol{u} \in \boldsymbol{U}$ such that

$$\tilde{a}(\boldsymbol{u}, \boldsymbol{v}) = (\boldsymbol{f}, \boldsymbol{v})_{L^2(\Omega)^d} \qquad \forall\, \boldsymbol{v} \in \boldsymbol{U}, \tag{26}$$

where $\tilde{a}(\boldsymbol{u}, \boldsymbol{v}) := (\underline{\underline{\sigma}}(\boldsymbol{u}), \underline{\underline{\varepsilon}}(\boldsymbol{v}))_{L^2(\Omega)^{d,d}}$. The well-posedness of the weak formulation (26) relies on Korn's inequality in $\boldsymbol{U}$ (cf., e.g., [1, Lemma 5.3.2]),

$$\|\boldsymbol{\nabla}\boldsymbol{v}\|_{L^2(\Omega)^{d,d}} \leqslant \sqrt{2}\|\underline{\underline{\varepsilon}}(\boldsymbol{v})\|_{L^2(\Omega)^{d,d}} \qquad \forall \boldsymbol{v} \in \boldsymbol{U}. \tag{27}$$

The use of Korn's inequality can be circumvented for the pure displacement problem using the following alternative Navier–Cauchy formulation: Find $\boldsymbol{u} \in \boldsymbol{U}$ such that

$$a(\boldsymbol{u}, \boldsymbol{v}) := (\mu\boldsymbol{\nabla}\boldsymbol{u}, \boldsymbol{\nabla}\boldsymbol{v})_{L^2(\Omega)^{d,d}} + ((\mu+\lambda)\boldsymbol{\nabla}\cdot\boldsymbol{u}, \boldsymbol{\nabla}\cdot\boldsymbol{v})_{L^2(\Omega)} = (\boldsymbol{f}, \boldsymbol{v})_{L^2(\Omega)^d} \qquad \forall \boldsymbol{v} \in \boldsymbol{U}. \tag{28}$$

This naturally coercive formulation is equivalent to (26) for homogeneous materials and pure Dirichlet boundary conditions. Throughout the rest of this section we focus on this alternative form. The treatment of mixed type boundary conditions is addressed in Section 4.2.5. We recall the following regularity result valid in $d = 2$; cf., e.g., [9, Lemma 2.2].

Lemma 14 (Regularity)**.** *Let $d = 2$ and assume that Ω is convex. Then, problem* (25) *has a unique solution $\boldsymbol{u} \in \boldsymbol{U}_* := \boldsymbol{U} \cap H^2(\Omega)^d$. Moreover, there exists a real $C_\mu > 0$ only depending on Ω and μ but not on λ, such that, for λ large enough,*

$$\mathcal{N}_{\mathrm{el}}(\boldsymbol{u}) := \|\boldsymbol{u}\|_{H^2(\Omega)^d} + |\lambda\boldsymbol{\nabla}\cdot\boldsymbol{u}|_{H^1(\Omega)} \leqslant C_\mu\|\boldsymbol{f}\|_{L^2(\Omega)^d}. \tag{29}$$

This implies, in particular, that, if $\lambda \to +\infty$, the divergence of the displacement field approaches zero, corresponding to a quasi-incompressible material; cf. [19] for a generalization to composite materials.

4.2.2 Discretization

Let $\mathcal{K}_h$ belong to an admissible mesh sequence in the sense of Definition 4. We consider an approximation of the displacement field in the space

$$\boldsymbol{U}_h := \mathfrak{CR}_0(\mathcal{K}_h)^d,$$

with $\mathfrak{CR}_0(\mathcal{K}_h)$ defined by (21). Henceforth we assume the choice $\eta = d$ in (9), so that the continuity of mean values stated in Lemma 8 holds. Lowest-order, locking-free discretizations of (25) satisfy an estimate of the form

$$\|\boldsymbol{u} - \boldsymbol{u}_h\|_{\mathrm{el}} \leqslant Ch\|\boldsymbol{f}\|_{L^2(\Omega)^d}, \tag{30}$$

where $\|\cdot\|_{\mathrm{el}}$ is a (discrete) energy norm and $C > 0$ is a constant possibly depending on μ and on the mesh regularity parameters but independent of h, λ, and $\boldsymbol{u}$. The key point is here that the multiplicative constant in the right-hand side of (30) does not blow up in the limit $\lambda \to +\infty$, i.e., the method converges uniformly in λ. To obtain (30) we prove that in general space dimension there holds with $\mathcal{N}_{\mathrm{el}}(\boldsymbol{u})$ defined by (29),

$$\|\boldsymbol{u} - \boldsymbol{u}_h\|_{\mathrm{el}} \leqslant C_{\mathrm{el}} h \mathcal{N}_{\mathrm{el}}(\boldsymbol{u}),$$

where $C_{\mathrm{el}} > 0$ has the same dependencies as C, and then invoke the regularity estimate in Lemma 14 to conclude in $d = 2$. The discrete problem reads: Find $\boldsymbol{u}_h \in \boldsymbol{U}_h$ such that

$$a_h(\boldsymbol{u}_h, \boldsymbol{v}_h) = (\boldsymbol{f}, \boldsymbol{v}_h)_{L^2(\Omega)^d} \qquad \forall\, \boldsymbol{v}_h \in \boldsymbol{U}_h, \tag{31}$$

with discrete bilinear form a_h such that

$$a_h(\boldsymbol{w}, \boldsymbol{v}) := (\mu \boldsymbol{\nabla}_h \boldsymbol{w}, \boldsymbol{\nabla}_h \boldsymbol{v})_{L^2(\Omega)^{d,d}} + (\mu \boldsymbol{\nabla}_h \cdot \boldsymbol{w}, \boldsymbol{\nabla}_h \cdot \boldsymbol{v})_{L^2(\Omega)} + (\lambda D_h(\boldsymbol{w}), D_h(\boldsymbol{v}))_{L^2(\Omega)}. \tag{32}$$

The last term in the right-hand side is treated using the discrete divergence D_h defined in Corollary 12 since the approximation properties of D_h are instrumental to ensure that λ only appears in terms of the form $|\lambda \boldsymbol{\nabla} \cdot \boldsymbol{u}|_{H^1(\Omega)}$ in the right-hand side of the error estimate (cf., in particular, the bound for the consistency term in the proof of Theorem 18).

Remark 15 (Implementation)**.** *In* (31)*, cell-centered unknowns for a given element $K \in \mathcal{K}_h$ are only linked with the face unknowns located on the boundary of K. As a result, they can be locally eliminated by taking the Schur complement of the corresponding block in the local matrix. This requires, in general, to inverse a $d \times d$ matrix. However, this cost can be further reduced by replacing in* (32) *the term $(\mu \boldsymbol{\nabla}_h \cdot \boldsymbol{u}_h, \boldsymbol{\nabla}_h \cdot \boldsymbol{v}_h)_{L^2(\Omega)}$ by $(\mu D_h(\boldsymbol{u}_h), D_h(\boldsymbol{v}_h))_{L^2(\Omega)}$. This choice avoids, without jeopardizing the approximation, the interaction of the cell unknowns for the different components of the displacement, hence the corresponding block of the local matrix is diagonal and trivial to invert.*

The energy norm associated to the bilinear form a_h is

$$\|\boldsymbol{v}\|_{\mathrm{el}}^2 := a_h(\boldsymbol{v}, \boldsymbol{v}) = \|\mu^{1/2} \boldsymbol{\nabla}_h \boldsymbol{v}\|_{L^2(\Omega)^{d,d}}^2 + \|\mu^{1/2} \boldsymbol{\nabla}_h \cdot \boldsymbol{v}\|_{L^2(\Omega)}^2 + \|\lambda^{1/2} D_h(\boldsymbol{v})\|_{L^2(\Omega)}^2. \tag{33}$$

Lemma 16 (Coercivity)**.** *There holds for all $\boldsymbol{v}_h \in \boldsymbol{U}_h$,*

$$a_h(\boldsymbol{v}_h, \boldsymbol{v}_h) = \|\boldsymbol{v}_h\|_{\mathrm{el}}^2 \geqslant \mu \|\boldsymbol{\nabla}_h \boldsymbol{v}_h\|_{L^2(\Omega)^{d,d}}^2.$$

The well-posedness of the discrete problem (31) then follows from the Lax–Milgram Lemma and Proposition 13. Let now $\boldsymbol{U}_{*h} := \boldsymbol{U}_* + \boldsymbol{U}_h$ with $\boldsymbol{U}_*$ defined in Lemma 14, and extend the bilinear form a_h to $\boldsymbol{U}_{*h} \times \boldsymbol{U}_{*h}$. Assuming $\boldsymbol{u} \in \boldsymbol{U}_*$ ensures that the boundary terms in the expression of the consistency error are well-defined, cf. Lemma 17. This additional regularity is verified, e.g., under the assumptions of Lemma 14.

Lemma 17 (Weak consistency)**.** *Let $\boldsymbol{u} \in \boldsymbol{U}$ denote the solution to* (28) *and additionally assume $\boldsymbol{u} \in \boldsymbol{U}_*$. Then, there holds for all $\boldsymbol{v}_h \in \boldsymbol{U}_h$,*

$$a_h(\boldsymbol{u}, \boldsymbol{v}_h) = (\boldsymbol{f}, \boldsymbol{v}_h)_{L^2(\Omega)^d} + \mathcal{E}_h(\boldsymbol{v}_h),$$

where, letting $\underline{\underline{\tau}}(\boldsymbol{u}) := \mu \boldsymbol{\nabla} \boldsymbol{u} + (\mu + \lambda)(\boldsymbol{\nabla} \cdot \boldsymbol{u}) \underline{\underline{I_d}}$,

$$\mathcal{E}_h(\boldsymbol{v}_h) := \sum_{F \in \mathcal{F}_{\mathcal{P}_h}} (\underline{\underline{\tau}}(\boldsymbol{u}) \boldsymbol{n}_F, [\![\boldsymbol{v}_h]\!])_{L^2(F)^d} + (\lambda(D_h(\boldsymbol{u}) - \boldsymbol{\nabla} \cdot \boldsymbol{u}), \boldsymbol{\nabla}_h \cdot \boldsymbol{v}_h)_{L^2(\Omega)}. \tag{34}$$

Proof. Observing that $(\lambda D_h(\boldsymbol{u}), D_h(\boldsymbol{v}_h))_{L^2(\Omega)} = (\lambda D_h(\boldsymbol{u}), \boldsymbol{\nabla}_h \cdot \boldsymbol{v}_h))_{L^2(\Omega)}$, and summing and subtracting $(\lambda \boldsymbol{\nabla} \cdot \boldsymbol{u}, \boldsymbol{\nabla}_h \cdot \boldsymbol{v}_h)_{L^2(\Omega)}$ from the right-hand side of (32) with $(\boldsymbol{w}, \boldsymbol{v}) = (\boldsymbol{u}, \boldsymbol{v}_h)$ yields

$$a_h(\boldsymbol{u}, \boldsymbol{v}_h) = (\underline{\underline{\tau}}(\boldsymbol{u}), \boldsymbol{\nabla}_h \boldsymbol{v}_h)_{L^2(\Omega)^{d,d}} + (\lambda(D_h(\boldsymbol{u}) - \boldsymbol{\nabla} \cdot \boldsymbol{u}), \boldsymbol{\nabla}_h \cdot \boldsymbol{v}_h)_{L^2(\Omega)}.$$

Integrating by parts the first term element-wise, rearranging the boundary contributions, and using $[\![\underline{\underline{\tau}}(\boldsymbol{u})]\!]_F \boldsymbol{n}_F = \boldsymbol{0}$ and $\{\underline{\underline{\tau}}(\boldsymbol{u})\}_F \boldsymbol{n}_F = \underline{\underline{\tau}}(\boldsymbol{u}) \boldsymbol{n}_F$ for all $F \in \mathcal{F}^{\mathrm{i}}_{\mathcal{P}_h}$, it is inferred

$$\begin{aligned}
(\underline{\underline{\tau}}(\boldsymbol{u}), \boldsymbol{\nabla}_h \boldsymbol{v}_h)_{L^2(\Omega)^{d,d}} &= -(\boldsymbol{\nabla} \cdot \underline{\underline{\tau}}(\boldsymbol{u}), \boldsymbol{v}_h)_{L^2(\Omega)^d} + \sum_{P \in \mathcal{P}_h} (\underline{\underline{\tau}}(\boldsymbol{u}) \boldsymbol{n}_P, \boldsymbol{v}_{h|P})_{L^2(\partial P)^d} \\
&= (\boldsymbol{f}, \boldsymbol{v}_h)_{L^2(\Omega)^d} + \sum_{F \in \mathcal{F}^{\mathrm{i}}_{\mathcal{P}_h}} ([\![\underline{\underline{\tau}}(\boldsymbol{u})]\!] \boldsymbol{n}_F, \{\boldsymbol{v}_h\})_{L^2(F)^d} + \sum_{F \in \mathcal{F}_{\mathcal{P}_h}} (\{\underline{\underline{\tau}}(\boldsymbol{u})\} \boldsymbol{n}_F, [\![\boldsymbol{v}_h]\!])_{L^2(F)^d} \\
&= (\boldsymbol{f}, \boldsymbol{v}_h)_{L^2(\Omega)^d} + \sum_{F \in \mathcal{F}_{\mathcal{P}_h}} (\underline{\underline{\tau}}(\boldsymbol{u}) \boldsymbol{n}_F, [\![\boldsymbol{v}_h]\!])_{L^2(F)^d},
\end{aligned}$$

where we have used $-\boldsymbol{\nabla} \cdot \underline{\underline{\tau}}(\boldsymbol{u}) = \boldsymbol{f}$ a.e. in Ω in the second line (cf. (28)). This concludes the proof. □

In the following theorem the continuity of mean values at interfaces plays an important role in estimating the boundary contribution in the consistency error.

Theorem 18 (Error estimate for (31))**.** *Let $\boldsymbol{u} \in \boldsymbol{U}$ denote the solution to* (28) *and additionally assume $\boldsymbol{u} \in \boldsymbol{U}_*$. Then, there exists $C_{\mathrm{el}} > 0$ independent of the meshsize, of λ, and of $\boldsymbol{u}$ such that, denoting by $\boldsymbol{u}_h \in \boldsymbol{U}_h$ the solution to* (31)*, there holds*

$$\|\boldsymbol{u} - \boldsymbol{u}_h\|_{\mathrm{el}} \leqslant C_{\mathrm{el}} h \mathcal{N}_{\mathrm{el}}(\boldsymbol{u}). \tag{35}$$

Proof. We note $a \lesssim b$ the inequality $a \leqslant Cb$ where $C > 0$ has the same dependence as the constant C_{el} in (35). The Cauchy–Schwarz inequality yields boundedness in the form $a_h(\boldsymbol{w}, \boldsymbol{v}) \leqslant \|\boldsymbol{w}\|_{\mathrm{el}} \|\boldsymbol{v}\|_{\mathrm{el}}$ for all $(\boldsymbol{w}, \boldsymbol{v}) \in \boldsymbol{U}_{*h} \times \boldsymbol{U}_{*h}$. This, together with Lemmata 16 and 17 and the Second Strang Lemma [32] (cf. also [24, Lemma 2.25]), yields:

$$\|\boldsymbol{u} - \boldsymbol{u}_h\|_{\mathrm{el}} \lesssim \inf_{\boldsymbol{v}_h \in \boldsymbol{U}_h} \|\boldsymbol{u} - \boldsymbol{v}_h\|_{\mathrm{el}} + \sup_{\boldsymbol{v}_h \in \boldsymbol{U}_h \setminus \{\boldsymbol{0}\}} \frac{|\mathcal{E}_h(\boldsymbol{v}_h)|}{\|\boldsymbol{v}_h\|_{\mathrm{el}}} := \mathfrak{T}_1 + \mathfrak{T}_2. \tag{36}$$

The first term in the right-hand side depends on the approximation properties of the discrete space in the $\|\cdot\|_{\mathrm{el}}$-norm, while the second is linked to the consistency error. Let $\boldsymbol{w}_h := \mathcal{I}_h^{\mathfrak{CR}}(\boldsymbol{u}) \in \boldsymbol{U}_h$. Using Lemma 10 twice and Corollary 12 respectively to treat the three terms in the right-hand side of (33) with $\boldsymbol{v} = \boldsymbol{u} - \boldsymbol{w}_h$ we infer,

$$\mathfrak{T}_1 \leqslant \|\boldsymbol{u} - \boldsymbol{w}_h\|_{\mathrm{el}} \lesssim h \|\boldsymbol{u}\|_{H^2(\Omega)^d} + h |\lambda^{1/2} \boldsymbol{\nabla} \cdot \boldsymbol{u}|_{H^1(\Omega)}. \tag{37}$$

To treat the consistency error, denote by $\mathfrak{T}_{2,1}$ and $\mathfrak{T}_{2,2}$ the two terms in the right-hand side of (34). Let

$$\underline{\underline{\phi_\mu}} := \mu(\boldsymbol{\nabla u} - \Pi_h^0(\boldsymbol{\nabla u})), \qquad \psi_s := s(\boldsymbol{\nabla}\cdot\boldsymbol{u} - \Pi_h^0(\boldsymbol{\nabla}\cdot\boldsymbol{u})), \text{ with } s \in \{\mu, \lambda\}.$$

Clearly, $\psi_\mu = \mathrm{tr}(\underline{\underline{\phi_\mu}})$. Using the continuity of mean values at interfaces together with the fact that both $\{\mu\Pi_h^0(\boldsymbol{\nabla u})\}_F$ and $\{s\Pi_h^0(\boldsymbol{\nabla}\cdot\boldsymbol{u})\}_F$, $s \in \{\mu, \lambda\}$, are constant on every $F \in \mathcal{F}_{\mathcal{P}_h}$, it is inferred

$$\begin{aligned}\mathfrak{T}_{2,1} &= \sum_{F\in\mathcal{F}_{\mathcal{P}_h}} (\{\underline{\underline{\tau}}(\boldsymbol{u}) - \Pi_h^0(\underline{\underline{\tau}}(\boldsymbol{u}))\}\boldsymbol{n}_F, [\![\boldsymbol{v}_h]\!] - \langle [\![\boldsymbol{v}_h]\!]\rangle_F)_{L^2(F)^d} \\ &= \sum_{F\in\mathcal{F}_{\mathcal{P}_h}} (\{\underline{\underline{\phi_\mu}} + \psi_\mu \underline{\underline{I_d}}\}\boldsymbol{n}_F, [\![\boldsymbol{v}_h]\!] - \langle [\![\boldsymbol{v}_h]\!]\rangle_F)_{L^2(F)^d} + \sum_{F\in\mathcal{F}_{\mathcal{P}_h}} (\{\psi_\lambda\}\boldsymbol{n}_F, [\![\boldsymbol{v}_h]\!] - \langle [\![\boldsymbol{v}_h]\!]\rangle_F)_{L^2(F)^d}.\end{aligned}$$

The Cauchy–Schwarz inequality followed by the trace inequality (5), the fact that the maximum number of faces of a pyramid is bounded uniformly in h, the approximation properties of the L^2-orthogonal projection, and (24) yield

$$\begin{aligned}\mathfrak{T}_{2,1} &\lesssim \left\{ \sum_{P\in\mathcal{P}_h} h \left(\|\underline{\underline{\phi_\mu}}|_P\|^2_{L^2(\partial P)^{d,d}} + \|\psi_{\lambda|P}\|^2_{L^2(\partial P)} \right) \right\}^{\frac{1}{2}} \times \left\{ \sum_{F\in\mathcal{F}_{\mathcal{P}_h}} h_F^{-1} \|[\![\boldsymbol{v}_h]\!] - \langle [\![\boldsymbol{v}_h]\!]\rangle_F\|^2_{L^2(F)^d} \right\}^{\frac{1}{2}} \\ &\lesssim h\mathcal{N}_{\mathrm{el}}(\boldsymbol{u})\|\boldsymbol{v}_h\|_{\mathrm{el}},\end{aligned} \tag{38}$$

where the bound $\|\boldsymbol{\nabla}_h\boldsymbol{v}_h\|_{L^2(\Omega)^{d,d}} \lesssim \|\boldsymbol{v}_h\|_{\mathrm{el}}$ is a consequence of Lemma 16. Finally, using the Cauchy–Schwarz inequality together with the approximation properties of the L^2-orthogonal projection and Lemma 16 it is inferred,

$$\mathfrak{T}_{2,2} \leqslant \|\lambda(\Pi_h^0(\boldsymbol{\nabla}\cdot\boldsymbol{u}) - \boldsymbol{\nabla}\cdot\boldsymbol{u})\|_{L^2(\Omega)}\|\boldsymbol{\nabla}_h\cdot\boldsymbol{v}_h\|_{L^2(\Omega)} \lesssim h|\lambda\boldsymbol{\nabla}\cdot\boldsymbol{u}|_{H^1(\Omega)}\|\boldsymbol{v}_h\|_{\mathrm{el}}. \tag{39}$$

Using inequalities (37), (38), and (39) to bound the right-hand side of (36) the conclusion follows. □

Corollary 19 (Uniform convergence with respect to λ in $d = 2$)**.** *If $d = 2$ the locking-free error estimate* (30) *holds with $C = C_{\mathrm{el}}C_\mu$.*

Remark 20 (Use of Lemma 14)**.** *In the proof of Theorem 18, the a priori bound on $|\lambda\boldsymbol{\nabla}\cdot\boldsymbol{u}|_{H^1(\Omega)}$ is only required to bound $\mathfrak{T}_2$. For $\mathfrak{T}_1$, the weaker regularity estimate $\|\boldsymbol{u}\|_{H^2(\Omega)^d} + |\lambda^{1/2}\boldsymbol{\nabla}\cdot\boldsymbol{u}|_{H^1(\Omega)} \lesssim \|\boldsymbol{f}\|_{L^2(\Omega)^d}$ is sufficient.*

Remark 21 (L^2-error estimate)**.** *Optimal error estimates for the L^2-error on the displacement can be derived using the Aubin–Nitsche trick based on the symmetry of the method.*

4.2.3 A numerical example: the closed cavity problem

To assess the robustness of the method (31) in the quasi-incompressible limit, we consider the closed cavity problem of Hansbo and Larson [29]. Although this problem does not exhibit the regularity required by Theorem 18, it is included as it is one of the simplest benchmarks for numerical locking. The implementation relies on the general framework recently introduced in [18], to which we refer for further details. We let $\Omega := (0,1)^2$, $\boldsymbol{f} \equiv \boldsymbol{0}$, and prescribe a horizontal displacement $\boldsymbol{u} = (1,0)$ on the upper side and $\boldsymbol{u} = (0,0)$ on the remaining three.

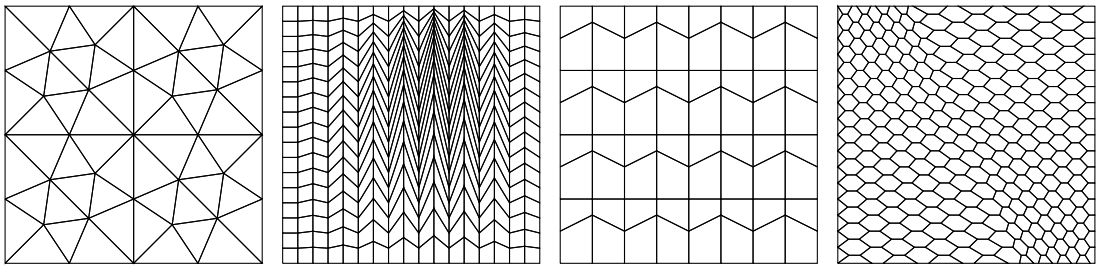

(a) Triangular (b) Kershaw (c) Trapezoidal (d) Hexagonal

Figure 3: Members of the mesh families for the numerical test of Section 4.2.3.

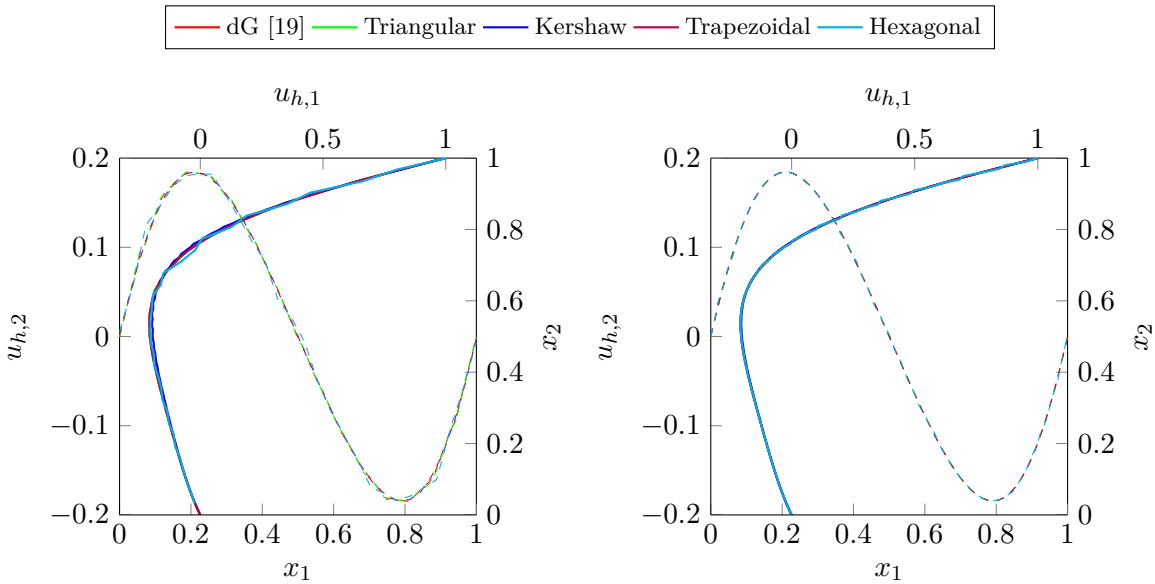

(a) Coarse meshes (b) Fine meshes

Figure 4: Results for the closed cavity problem on a coarse and a fine mesh extracted from the mesh families of Figure 3. *Solid lines:* horizontal displacement $u_{h,1}$ along the vertical centerline. *Dashed lines:* vertical displacement $u_{h,2}$ along the horizontal centerline.

The elastic modulus and Poisson's ratio are chosen as $E = 1000$ and $\nu = 0.4999$ respectively. The Lamé parameters can be derived from the relations $\lambda = \frac{\nu E}{(1+\nu)(1-2\nu)}$, $\mu = \frac{E}{2(1+\nu)}$, which show, in particular, that $\lambda \to +\infty$ as $\nu \to 1/2$. The discrete problem (31) is solved on the four mesh sequences depicted in Figure 3. From each mesh family, a coarse and a fine meshes are selected featuring roughly the same number of elements. Figure 4 depicts the values of the horizontal displacement $u_{h,1}$ along the vertical centerline $x_1 = 1/2$ as well as the values of the vertical displacement $u_{h,2}$ along the horizontal centerline $x_2 = 1/2$. The results of the (more expensive) dG method of [19] on the matching triangular mesh are also included for comparison. As predicted, no sign of numerical locking is observed.

4.2.4 Variations and links with finite volume and finite element methods

Flux formulation and local conservation Following [25, Section 2.4] it is possible to reformulate the discrete bilinear form (32) in terms of numerical fluxes. More specifically, introducing $\mathbb{U}_h := \mathbb{V}_{h,0}^d$ where $\mathbb{V}_{h,0}$ is defined by (21), let $\boldsymbol{w}_h$, $\boldsymbol{v}_h \in \boldsymbol{U}_h$ be two discrete functions

and denote by $\mathbb{w}_h = (\mathbb{w}_{h,i})_{1\leqslant i\leqslant d} \in \mathbb{U}_h$ and $\mathbb{v}_h = (\mathbb{v}_{h,i})_{1\leqslant i\leqslant d} \in \mathbb{U}_h$ the corresponding vectors of DOFs, where, for all $i \in \{1,\dots,d\}$, $\mathbb{w}_{h,i}$ and $\mathbb{v}_{h,i}$ are the vectors of DOFs associated to the ith components of $\boldsymbol{w}_h$ and $\boldsymbol{v}_h$ respectively. Our goal is to show that there exists a family of numerical fluxes $(\boldsymbol{\Phi}_{K,F}(\mathbb{w}_h))_{K\in\mathcal{K}_h,\,F\in\mathcal{F}_K}$ with $\boldsymbol{\Phi}_{K,F}(\mathbb{w}_h) = (\Phi_{K,F,i}(\mathbb{w}_h))_{1\leqslant i\leqslant d}$ such that

$$a_h(\boldsymbol{w}_h,\boldsymbol{v}_h) = \sum_{i=1}^{d}\sum_{K\in\mathcal{K}_h}\sum_{F\in\mathcal{F}_K}\Phi_{K,F,i}(\mathbb{w}_h)(v_{F,i}-v_{K,i}), \tag{40}$$

with a_h defined by (32). The main interest of this alternative formulation is that it allows to prove a local conservation property similar to those encountered in standard finite volume methods. Recalling the expression (40) for the bilinear form a_h and using the cell center as a quadrature node to approximate the right-hand side in each element, the discrete problem (31) in algebraic form reads: Find $\mathbb{u}_h \in \mathbb{U}_h$ such that for all $\mathbb{v}_h \in \mathbb{U}_h$ there holds,

$$\sum_{i=1}^{d}\sum_{K\in\mathcal{K}_h}\sum_{F\in\mathcal{F}_K}\Phi_{K,F,i}(\mathbb{u}_h)(v_{F,i}-v_{K,i}) = \sum_{i=1}^{d}\sum_{K\in\mathcal{K}_h}|K|\,f_i(\boldsymbol{x}_K)v_{K,i}. \tag{41}$$

Consider now an interface $F \in \mathcal{F}^{\mathrm{i}}_{\mathcal{K}_h}$ such that $F \subset \partial K_1 \cap \partial K_2$, and let $\mathbb{v}_{h,i}$ be such that $v_{F,i} = 1$, $v_{F',i} = 0$ for all $F' \in \mathcal{F}_{\mathcal{K}_h}\backslash\{F\}$, and $v_{K,i} = 0$ for all $K \in \mathcal{K}_h$. There follows from (41),

$$\Phi_{K_1,F,i}(\mathbb{u}_h) = -\Phi_{K_2,F,i}(\mathbb{u}_h), \tag{42}$$

i.e., the method is locally conservative. An important remark is that the loading term does not appear in (42) since its approximation in (41) only involves cell DOFs.

Proposition 22 (Flux formulation)**.** *For all $\boldsymbol{w}_h$, $\boldsymbol{v}_h \in \boldsymbol{U}_h$, the flux formulation* (40) *is obtained setting for all $K \in \mathcal{K}_h$, $F \in \mathcal{F}_K$, and $i \in \{1,\dots,d\}$,*

$$\Phi_{K,F,i}(\mathbb{w}_h) := \sum_{F'\in\mathcal{F}_K}|K_{F'}|\left[\mu\boldsymbol{G}_{K_{F'}}(\mathbb{w}_{h,i})\cdot\boldsymbol{y}^K_{F',F} + \left(\sum_{j=1}^{d}\mu\boldsymbol{G}_{K_{F'}}(\mathbb{w}_{h,j}) + \lambda\boldsymbol{G}_K(\mathbb{w}_{h,j})\right)\cdot\boldsymbol{e}_j\left(\boldsymbol{y}^K_{F',F}\cdot\boldsymbol{e}_i\right)\right],$$

where $\mathbb{w}_h$, $\mathbb{v}_h \in \mathbb{U}_h$ are the vectors of DOFs associated to $\boldsymbol{w}_h$ and $\boldsymbol{v}_h$ respectively, $(\boldsymbol{e}_i)_{1\leqslant i\leqslant d}$ denotes the canonical basis of $\mathbb{R}^d$, and

$$\boldsymbol{y}^K_{F',F} := \begin{cases} \frac{|F|}{|K|}\boldsymbol{n}_{K,F} + \frac{\eta}{d_{K,F}}\left(1 - \frac{|F|}{|K|}\boldsymbol{n}_{K,F}\cdot(\overline{\boldsymbol{x}}_F - \boldsymbol{x}_K)\right)\boldsymbol{n}_{K,F} & \text{if } F = F', \\ \frac{|F|}{|K|}\boldsymbol{n}_{K,F} - \frac{\eta}{d_{K,F'}|K|}\,|F|\,\boldsymbol{n}_{K,F}\cdot(\overline{\boldsymbol{x}}_{F'} - \boldsymbol{x}_K)\boldsymbol{n}_{K,F'} & \text{otherwise.} \end{cases} \tag{43}$$

Proof. For all $\mathbb{v}_h \in \mathbb{V}_h$, all $K \in \mathcal{K}_h$, and all $F' \in \mathcal{F}_K$ there holds with $\boldsymbol{G}_{K_{F'}}(\mathbb{v}_h)$ defined by (8) (cf. [25, eq. (26) et seq.]),

$$\boldsymbol{G}_{K_{F'}}(\mathbb{v}_h) = \sum_{F\in\mathcal{F}_K}\boldsymbol{y}^K_{F',F}\,(v_F - v_K)\,. \tag{44}$$

Using (8) and (10), and observing that $(\lambda D_h(\boldsymbol{w}_h), D_h(\boldsymbol{v}_h))_{L^2(\Omega)} = (\lambda D_h(\boldsymbol{w}_h), \boldsymbol{\nabla}_h\cdot\boldsymbol{v}_h)_{L^2(\Omega)}$ owing to (20) together with the properties of the L^2-orthogonal projector, it is inferred

$$a_h(\boldsymbol{w}_h,\boldsymbol{v}_h) = \sum_{i=1}^{d}\sum_{K\in\mathcal{K}_h}\sum_{F'\in\mathcal{F}_K}|K_{F'}|\left[\mu\boldsymbol{G}_{K_{F'}}(\mathbb{w}_{h,i}) + \left(\sum_{j=1}^{d}\mu\boldsymbol{G}_{K_{F'}}(\mathbb{w}_{h,j})\cdot\boldsymbol{e}_j + \lambda\boldsymbol{G}_K(\mathbb{w}_{h,j})\cdot\boldsymbol{e}_j\right)\boldsymbol{e}_i\right]\cdot\boldsymbol{G}_{K_{F'}}(\mathbb{v}_{h,i}).$$

The conclusion follows using the expression (44) for $\boldsymbol{G}_{K_{F'}}(\mathbb{v}_{h,i})$ and exchanging the sums of indices F and F'. □

Link with the Crouzeix–Raviart solution on matching simplicial meshes Assume that $\mathcal{K}_h$ is a matching simplicial mesh and let

$$\mathbb{CR}_0(\mathcal{K}_h) := \{v_h \in \mathbb{CR}(\mathcal{K}_h) \mid v_h(\overline{\boldsymbol{x}}_F) = 0, \forall F \in \mathcal{F}^{\mathrm{b}}_{\mathcal{K}_h}\},$$

and $\hat{\boldsymbol{U}}_h := \mathbb{CR}_0(\mathcal{K}_h)^d$. We show in this section that a suitable modification of the right-hand side allows to recover the Crouzeix–Raviart solution $\hat{\boldsymbol{u}}_h \in \hat{\boldsymbol{U}}_h$ such that (cf. [9]),

$$a_h(\hat{\boldsymbol{u}}_h, \boldsymbol{v}_h) = (\boldsymbol{f}, \boldsymbol{v}_h)_{L^2(\Omega)^d} \qquad \forall \boldsymbol{v}_h \in \hat{\boldsymbol{U}}_h. \tag{45}$$

Let $W(\mathcal{P}_h) := \{v \in H^1(\mathcal{P}_h) \mid \langle [\![v]\!] \rangle_F = 0 \text{ for all } F \in \mathcal{F}^{\mathrm{i}}_{\mathcal{P}_h}\}$, and denote by $\mathcal{I}_h^{\mathbb{CR}} : W(\mathcal{P}_h) \to \mathbb{CR}(\mathcal{K}_h)$ the interpolator that maps a function $v \in W(\mathcal{P}_h)$ on the function $v_h := \mathcal{I}_h^{\mathbb{CR}}(v) \in \mathbb{CR}(\mathcal{K}_h)$ such that $v_h(\overline{\boldsymbol{x}}_F) = \langle v \rangle_F$ for all $F \in \mathcal{F}_{\mathcal{K}_h}$. We consider the following variation of (31): Find $\boldsymbol{u}_h \in \boldsymbol{U}_h$ such that

$$a_h(\boldsymbol{u}_h, \boldsymbol{v}_h) = (\boldsymbol{f}, \mathcal{I}_h^{\mathbb{CR}}(\boldsymbol{v}_h))_{L^2(\Omega)^d} \qquad \forall \boldsymbol{v}_h \in \boldsymbol{U}_h, \tag{46}$$

where the sole difference with respect to (31) lies in the treatment of the right-hand side.

Lemma 23 (Relation between (45) and (46))**.** *There holds* $\boldsymbol{u}_h = \hat{\boldsymbol{u}}_h$.

Proof. Let $\mathbb{U}_h \ni \hat{\mathbb{u}}_h = (\hat{\mathbb{u}}_{h,i})_{1 \leqslant i \leqslant d}$ be such that, for $i \in \{1, \dots, d\}$,

$$\hat{\mathbb{u}}_{h,i} = ((\hat{u}_{h,i}(\boldsymbol{x}_K))_{K \in \mathcal{K}_h}, (\hat{u}_{h,i}(\overline{\boldsymbol{x}}_F))_{F \in \mathcal{F}_{\mathcal{K}_h}}) \in \mathbb{V}_{h,0}.$$

Clearly, for all $K \in \mathcal{K}_h$, all $F \in \mathcal{F}_K$, and all $i \in \{1, \dots, d\}$, $\boldsymbol{R}_{K_F}(\hat{\mathbb{u}}_{h,i}) = \boldsymbol{0}$, hence $\boldsymbol{G}_{K_F}(\hat{\mathbb{u}}_{h,i}) = \boldsymbol{G}_K(\hat{\mathbb{u}}_{h,i}) = (\boldsymbol{\nabla}_h \hat{u}_{h,i})_{|K}$. As a consequence, $\hat{\boldsymbol{u}}_h = \mathfrak{R}_h(\hat{\mathbb{u}}_h)$. Accounting for this fact, there holds for all $\boldsymbol{v}_h \in \boldsymbol{U}_h$ such that $\boldsymbol{v}_h = \mathfrak{R}_h(\mathbb{v}_h)$ with $\mathbb{v}_h \in \mathbb{U}_h$,

$$\begin{aligned}
a_h(\hat{\boldsymbol{u}}_h, \boldsymbol{v}_h) &= \sum_{i=1}^d \sum_{K \in \mathcal{K}_h} \sum_{F \in \mathcal{F}_K} |K_F| \Big\{ \mu \boldsymbol{G}_K(\hat{\mathbb{u}}_{h,i}) \cdot \boldsymbol{G}_{K_F}(\mathbb{v}_{h,i}) + \mu \boldsymbol{G}_K(\hat{\mathbb{u}}_{h,i}) \cdot \boldsymbol{e}_i D_{K_F}(\mathbb{v}_h) \\
&\qquad + \lambda \boldsymbol{G}_K(\hat{\mathbb{u}}_{h,i}) \cdot \boldsymbol{e}_i D_K(\mathbb{v}_h) \Big\} \\
&= \sum_{i=1}^d \sum_{K \in \mathcal{K}_h} |K| \Big\{ \mu \boldsymbol{G}_K(\hat{\mathbb{u}}_{h,i}) \cdot \boldsymbol{G}_K(\mathbb{v}_{h,i}) + (\mu + \lambda) \boldsymbol{G}_K(\hat{\mathbb{u}}_{h,i}) \cdot \boldsymbol{e}_i D_K(\mathbb{v}_h) \Big\} \\
&= a_h(\hat{\boldsymbol{u}}_h, \mathcal{I}_h^{\mathbb{CR}}(\boldsymbol{v}_h)) = (\boldsymbol{f}, \mathcal{I}_h^{\mathbb{CR}}(\boldsymbol{v}_h))_{L^2(\Omega)^d},
\end{aligned}$$

where the first passage is a consequence of (17) and we have let, for the sake of conciseness $D_K(\mathbb{v}_h) := \sum_{j=1}^d \boldsymbol{G}_K(\mathbb{v}_{h,j}) \cdot \boldsymbol{e}_j$ and $D_{K_F}(\mathbb{v}_h) := \sum_{j=1}^d \boldsymbol{G}_{K_F}(\mathbb{v}_{h,j}) \cdot \boldsymbol{e}_j$. Owing to the coercivity of a_h, problem (46) admits a unique solution and we therefore conclude that $\hat{\boldsymbol{u}}_h = \boldsymbol{u}_h$. □

4.2.5 Mixed type boundary conditions

We describe here a possible modification of the method that allows to account for homogeneous mixed type boundary conditions (the generalization to the nonhomogeneous case is straightforward). The continuous problem reads

$$\begin{aligned}
-\boldsymbol{\nabla} \cdot \underline{\underline{\sigma}}(\boldsymbol{u}) &= \boldsymbol{f} && \text{in } \Omega, \\
\boldsymbol{u} &= \boldsymbol{0} && \text{on } \partial\Omega^{\mathrm{D}}, \\
\underline{\underline{\sigma}}(\boldsymbol{u}) \boldsymbol{n} &= \boldsymbol{0} && \text{on } \partial\Omega^{\mathrm{N}},
\end{aligned} \tag{47}$$

where $\partial\Omega^{\mathrm{D}}$ and $\partial\Omega^{\mathrm{N}}$ are such that $\partial\Omega^{\mathrm{D}} \neq \varnothing$, $\partial\Omega^{\mathrm{D}} \cap \partial\Omega^{\mathrm{N}} = \varnothing$, and $\partial\Omega^{\mathrm{D}} \cup \partial\Omega^{\mathrm{N}} = \partial\Omega$. Let $\boldsymbol{U} := H^1_{\mathrm{D}}(\Omega)^d$ with $H^1_{\mathrm{D}}(\Omega) := \{v \in H^1(\Omega) \mid v_{|\partial\Omega^{\mathrm{D}}} = 0\}$. In this case, the weak formulation (28) is no longer equivalent to the continuous problem (47), and (26) must be used instead: Find $\boldsymbol{u} \in \boldsymbol{U}$ such that

$$\tilde{a}(\boldsymbol{u}, \boldsymbol{v}) = (\boldsymbol{f}, \boldsymbol{v})_{L^2(\Omega)^d} \qquad \forall\, \boldsymbol{v} \in \boldsymbol{U}. \tag{48}$$

The well-posedness of the weak formulation (48) relies on Korn's inequality (27), which is still valid on the space $H^1_{\mathrm{D}}(\Omega)^d$ (up to a multiplicative constant depending on $\partial\Omega^{\mathrm{D}}$). Likewise, the regularity estimate of Lemma 14 holds for problem (47) in the case of a convex polygonal domain with the above definition of $\boldsymbol{U}$ and $\boldsymbol{U}_* := \boldsymbol{U} \cap H^2(\Omega)^d$. We introduce the following H^1_{D}-like discrete space to approximate the displacement field:

$$\mathfrak{CR}_{\mathrm{D}}(\mathcal{K}_h) := \mathfrak{R}_h(\mathbb{V}_{h,\mathrm{D}}), \qquad \mathbb{V}_{h,\mathrm{D}} = \{\mathbb{v}_h \in \mathbb{V}_h \mid v_F = 0,\, \forall F \in \mathcal{F}^{\mathrm{b,D}}_{\mathcal{K}_h}\},$$

where $\mathcal{F}^{\mathrm{b,D}}_{\mathcal{K}_h} := \{F \in \mathcal{F}^{\mathrm{b}}_{\mathcal{K}_h} \mid F \subset \partial\Omega^{\mathrm{D}}\}$. We also introduce the set $\mathcal{F}^{\mathrm{b,N}}_{\mathcal{K}_h} := \mathcal{F}^{\mathrm{b}}_{\mathcal{K}_h} \backslash \mathcal{F}^{\mathrm{b,D}}_{\mathcal{K}_h}$. We first note that $\|\boldsymbol{\nabla}_h v_h\|_{L^2(\Omega)^d}$ is still a norm on $\mathfrak{CR}_{\mathrm{D}}(\mathcal{K}_h)$. Owing to the nonconformity of the space we consider, Korn's inequality only holds in the following generalized sense (cf. [7, eq. (1.12)]):

$$\|\boldsymbol{\nabla}_h \boldsymbol{v}\|_{L^2(\Omega)^{d,d}} \leqslant C_{\mathrm{K}} \left(\|\underline{\underline{\varepsilon_h}}(\boldsymbol{v})\|^2_{L^2(\Omega)^{d,d}} + |\boldsymbol{v}|^2_{\mathrm{J,D}} \right)^{\frac{1}{2}},$$

for any $\boldsymbol{v} = (v_i)_{1 \leqslant i \leqslant d} \in H^1(\mathcal{P}_h)^d$, where $C_{\mathrm{K}} > 0$ is independent of the meshsize (but depends on Ω and on the mesh regularity parameters), and $|\boldsymbol{v}|^2_{\mathrm{J,D}} := \sum_{i=1}^d |v_i|^2_{\mathrm{J,D}}$ with $|v|^2_{\mathrm{J,D}} := \sum_{F \in \mathcal{F}_{\mathcal{P}_h} \backslash \mathcal{F}^{\mathrm{b,N}}_{\mathcal{K}_h}} h_F^{-1} \|[\![v]\!]\|^2_{L^2(F)}$. A completely analogous difficulty arises for the standard Crouzeix–Raviart space. To overcome this problem, we take inspiration from [29] and consider a discrete version of the bilinear form $\tilde{a}$ which incorporates a least-square penalization of jumps. More specifically, letting $\boldsymbol{U}_h := \mathfrak{CR}_{\mathrm{D}}(\mathcal{K}_h)^d$, the discrete problem reads: Find $\boldsymbol{u}_h \in \boldsymbol{U}_h$ such that

$$\tilde{a}_h(\boldsymbol{u}_h, \boldsymbol{v}_h) = (\boldsymbol{f}, \boldsymbol{v}_h)_{L^2(\Omega)^d} \qquad \forall\, \boldsymbol{v}_h \in \boldsymbol{U}_h, \tag{49}$$

where the discrete bilinear form $\tilde{a}_h$ is given by

$$\tilde{a}_h(\boldsymbol{w}, \boldsymbol{v}) := (2\mu \underline{\underline{\varepsilon_h}}(\boldsymbol{w}), \underline{\underline{\varepsilon_h}}(\boldsymbol{v}))_{L^2(\Omega)^{d,d}} + (\lambda D_h(\boldsymbol{w}), D_h(\boldsymbol{v}))_{L^2(\Omega)} + \sum_{F \in \mathcal{F}_{\mathcal{P}_h} \backslash \mathcal{F}^{\mathrm{b,N}}_{\mathcal{K}_h}} h_F^{-1} (2\mu [\![\boldsymbol{w}]\!], [\![\boldsymbol{v}]\!])_{L^2(F)^d}. \tag{50}$$

It is worth observing that, while the idea of penalizing jumps to recover a discrete Korn's inequality appears natural in the present approach, this is not the case in other related frameworks for which the notion of affine reconstruction does not necessarily make sense.

Remark 24 (Implementation)**.** *We stress that in this case it is not possible to integrate the penalty term in* (50) *using the face barycenter as a quadrature point, since this would yield a vanishing contribution. A quadrature rule exact for polynomials of degree at least 2 must be used instead. Also, the penalty term establishes a link between the cell unknowns of neighboring elements. As a result, it is no longer possible to formulate the method in terms of face unknowns only as for the pure displacement problem; cf. Remark 15.*

The energy norm associated to the bilinear form $\tilde{a}_h$ is

$$\|\boldsymbol{v}\|^2_{\mathrm{el}} := \tilde{a}_h(\boldsymbol{v}, \boldsymbol{v}) = \|(2\mu)^{1/2} \underline{\underline{\varepsilon_h}}(\boldsymbol{v})\|^2_{L^2(\Omega)^{d,d}} + \|\lambda^{1/2} D_h(\boldsymbol{v})\|^2_{L^2(\Omega)} + |(2\mu)^{1/2} \boldsymbol{v}|^2_{\mathrm{J,D}}. \tag{51}$$

Lemma 25 (Coercivity)**.** *There holds for all* $\boldsymbol{v}_h \in \boldsymbol{U}_h$*,*

$$\tilde{a}_h(\boldsymbol{v}_h, \boldsymbol{v}_h) = \|\boldsymbol{v}_h\|_{\mathrm{el}}^2 \geqslant 2\mu C_{\mathrm{K}}^{-2} \|\boldsymbol{\nabla}_h \boldsymbol{v}_h\|_{L^2(\Omega)^{d,d}}^2.$$

The well-posedness of problem (49) is now straightforward. Defining $\boldsymbol{U}_{*h} := \boldsymbol{U}_* + \boldsymbol{U}_h$ and extending $\tilde{a}_h$ to $\boldsymbol{U}_{*h} \times \boldsymbol{U}_{*h}$, the convergence analysis can be carried out in a similar way as in Section 4.2.2. Assuming $\boldsymbol{u} \in \boldsymbol{U}_*$, the consistency error becomes, for all $\boldsymbol{v}_h \in \boldsymbol{U}_h$,

$$\mathcal{E}_h(\boldsymbol{v}_h) := \sum_{F \in \mathcal{F}_{\mathcal{P}_h} \setminus \mathcal{F}_{\mathcal{K}_h}^{\mathrm{b,N}}} (\underline{\sigma}(\boldsymbol{u})\boldsymbol{n}_F, [\![\boldsymbol{v}_h]\!])_{L^2(F)^d} + (\lambda(D_h(\boldsymbol{u}) - \boldsymbol{\nabla}\cdot\boldsymbol{u}), \boldsymbol{\nabla}_h\cdot\boldsymbol{v}_h)_{L^2(\Omega)}.$$

Using the same notation as in the proof of Theorem 18, with $\boldsymbol{w}_h := \mathcal{I}_h^{\mathfrak{CR}}(\boldsymbol{u}) \in \boldsymbol{U}_h$, the term $\mathfrak{T}_1$ can be handled as

$$\mathfrak{T}_1 \leqslant \|\boldsymbol{u} - \boldsymbol{w}_h\|_{\mathrm{el}} \lesssim h\|\boldsymbol{u}\|_{H^2(\Omega)^d} + h|\lambda^{1/2}\boldsymbol{\nabla}\cdot\boldsymbol{u}|_{H^1(\Omega)},$$

using Lemma 10, Corollary 12, and the trace inequality (6) with $\mathcal{S}_h = \mathcal{P}_h$ combined with Lemma 10, respectively to treat the three terms in the right-hand side of (51) with $\boldsymbol{v} = \boldsymbol{u} - \boldsymbol{w}_h$. The remaining terms can be treated by using exactly the same arguments as in the proof of Theorem 18. As a result, if $d = 2$, we again obtain a locking-free error estimate of the form (30).

4.3 Stokes: inf-sup stability and large irrotational body forces

In this section we briefly discuss an inf-sup stable method for the Stokes problem with velocity components in $\mathfrak{CR}(\mathcal{K}_h)$ and piecewise constant pressure. We also pinpoint a general strategy for the treatment of large irrotational forces and apply it to the proposed method.

4.3.1 Setting and discretization

The link between locking-free approximations of linear elasticity and inf-sup stable approximations of the Stokes problem is well-known; cf., e.g., the discussion in [10, Section VI.3]. We consider here a Newtonian fluid of constant unit viscosity whose motion is governed by the Stokes equations,

$$\begin{aligned} -\triangle\boldsymbol{u} + \boldsymbol{\nabla}p &= \boldsymbol{f} && \text{in } \Omega, \\ \boldsymbol{\nabla}\cdot\boldsymbol{u} &= 0 && \text{in } \Omega, \\ \boldsymbol{u} &= \boldsymbol{0} && \text{on } \partial\Omega, \\ \int_\Omega p &= 0, \end{aligned} \tag{52}$$

where $\boldsymbol{f} \in L^2(\Omega)^d$ represents the volumetric body force acting on the fluid. Let $\boldsymbol{U} := H_0^1(\Omega)^d$, and $P := L_0^2(\Omega)$ with $L_0^2(\Omega) := \{q \in L^2(\Omega) \mid \int_\Omega q = 0\}$. The weak formulation of problem (52) reads: Find $(\boldsymbol{u}, p) \in \boldsymbol{U} \times P$ such that

$$a(\boldsymbol{u}, \boldsymbol{v}) + b(\boldsymbol{v}, p) - b(\boldsymbol{u}, q) = (\boldsymbol{f}, \boldsymbol{v})_{L^2(\Omega)^d} \qquad \forall (\boldsymbol{v}, q) \in \boldsymbol{U} \times P, \tag{53}$$

where $a(\boldsymbol{u}, \boldsymbol{v}) := (\boldsymbol{\nabla}\boldsymbol{u}, \boldsymbol{\nabla}\boldsymbol{v})_{L^2(\Omega)^{d,d}}$ and $b(\boldsymbol{v}, p) := -(\boldsymbol{\nabla}\cdot\boldsymbol{v}, p)_{L^2(\Omega)}$. To approximate (53), let $\mathcal{K}_h$ belong to an admissible mesh sequence and define the following discrete spaces:

$$\boldsymbol{U}_h := \mathfrak{CR}_0(\mathcal{K}_h)^d, \qquad P_h := \mathbb{P}_d^0(\mathcal{K}_h) \cap L_0^2(\Omega).$$

We equip $\boldsymbol{U}_h$ with the norm $\|\boldsymbol{v}\|_{\boldsymbol{U}} := \|\boldsymbol{\nabla}_h\boldsymbol{v}\|_{L^2(\Omega)^{d,d}}$, see Proposition 13, and P_h with the norm $\|q\|_P := \|q\|_{L^2(\Omega)}$. We assume in the following $\eta = d$ in (9), so that the continuity of mean values

stated in Lemma 8 holds, and consider the following discrete problem: Find $(\boldsymbol{u}_h, p_h) \in \boldsymbol{U}_h \times P_h$ such that

$$a_h(\boldsymbol{u}_h, \boldsymbol{v}_h) + b_h(\boldsymbol{v}_h, p_h) - b_h(\boldsymbol{u}_h, q_h) = (\boldsymbol{f}, \boldsymbol{v}_h)_{L^2(\Omega)^d} \qquad \forall (\boldsymbol{v}_h, q_h) \in \boldsymbol{U}_h \times P_h, \tag{54}$$

where $a_h(\boldsymbol{w}, \boldsymbol{v}) := (\boldsymbol{\nabla}_h \boldsymbol{w}, \boldsymbol{\nabla}_h \boldsymbol{v})_{L^2(\Omega)^{d,d}}$ and $b_h(\boldsymbol{v}, q) := -(\boldsymbol{\nabla}_h \cdot \boldsymbol{v}, q)_{L^2(\Omega)}$. For all $(\boldsymbol{v}_h, q_h) \in \boldsymbol{U}_h \times P_h$ there holds

$$b_h(\boldsymbol{v}_h, q_h) = -(D_h(\boldsymbol{v}_h), q_h)_{L^2(\Omega)}. \tag{55}$$

Lemma 26 (inf-sup stability for b_h)**.** *There exists $\beta > 0$ independent of the meshsize, such that, for all $q_h \in P_h$,*

$$\beta \|q_h\|_P \leqslant \sup_{\boldsymbol{w}_h \in \boldsymbol{U}_h \setminus \{\boldsymbol{0}\}} \frac{b_h(\boldsymbol{w}_h, q_h)}{\|\boldsymbol{w}_h\|_{\boldsymbol{U}}}. \tag{56}$$

Proof. We sketch the proof for the sake of completeness. Let $\boldsymbol{v} \in \boldsymbol{U}$ and $\boldsymbol{v}_h := \mathcal{I}_h^{\mathfrak{CR}}(\boldsymbol{v}) \in \boldsymbol{U}_h$. Using the triangular inequality followed by (16) with $l = 0$, it is inferred with C independent of the meshsize, $\|\boldsymbol{v}_h\|_{\boldsymbol{U}} \leqslant \|\boldsymbol{\nabla} \boldsymbol{v} - \boldsymbol{\nabla}_h \boldsymbol{v}_h\|_{L^2(\Omega)^{d,d}} + \|\boldsymbol{\nabla} \boldsymbol{v}\|_{L^2(\Omega)^{d,d}} \leqslant C \|\boldsymbol{v}\|_{H^1(\Omega)^d}$. This H^1-stability property together with Corollary 12 and (55) show that $\mathcal{I}_h^{\mathfrak{CR}}$ can play the role of a Fortin operator, and (56) results from an application of [10, Proposition II.8]. □

The well-posedness of the discrete problem (54) follows from Lemma 26 together with the coercivity of a_h (an immediate consequence of Proposition 13). Moreover, as pointed out in [10, Section IV.3], the inf-sup condition proved in Lemma 26 is intimately linked to the good behavior of the method (31) in the quasi-incompressible limit. In fact, for inf-sup stable approximations of the Stokes problem with discontinuous pressures, one can obtain a locking-free primal method for the pure displacement problem of elasticity by performing static condensation of pressures, which is equivalent to introducing a projection on divergence terms (this strategy can e.g. be pursued for the method of [5, 6]).

Using classical arguments, one can prove the following result, which is invoked in the discussion of Section 4.3.3. As in Theorem 18, the continuity of mean values at interfaces is used to bound the consistency error. Optimal error estimates for the L^2-error on the velocity can also be derived using the Aubin–Nitsche trick.

Theorem 27 (Error estimate for (54))**.** *Assume $\boldsymbol{u} \in \boldsymbol{U} \cap H^2(\Omega)^d$ and $p \in P \cap H^1(\Omega)$. Then, there holds with $C > 0$ independent of the meshsize, of $\boldsymbol{u}$, and of p,*

$$\|(\boldsymbol{u} - \boldsymbol{u}_h, p - p_h)\|_{\mathrm{sto}} \leqslant C h \mathcal{N}_{\mathrm{sto}}(\boldsymbol{u}, p),$$

where $\|(\boldsymbol{v}, q)\|_{\mathrm{sto}}^2 := \|\boldsymbol{v}\|_{\boldsymbol{U}}^2 + \|q\|_P^2$ and $\mathcal{N}_{\mathrm{sto}}(\boldsymbol{u}, p) := \|\boldsymbol{u}\|_{H^2(\Omega)^d} + \|p\|_{H^1(\Omega)}$.

4.3.2 Variations and links with finite volume and finite element methods

Flux formulation and local conservation Let $(\boldsymbol{w}_h, r_h), (\boldsymbol{v}_h, q_h) \in \boldsymbol{U}_h \times P_h$ be two discrete functions, and denote by $(\mathbb{w}_h, \mathbb{r}_h), (\mathbb{v}_h, \mathbb{q}_h) \in \mathbb{U}_h \times \mathbb{P}_h$ the corresponding vectors of DOFs, where we have set $\mathbb{U}_h := \mathbb{V}_{h,0}^d$ and $\mathbb{P}_h := \{\mathbb{q}_h \in \mathbb{R}^{\mathcal{K}_h} \mid \sum_{K \in \mathcal{K}_h} |K| \, q_K = 0\}$. Then, proceeding as in Section 4.2.4, one can show that for the two families of fluxes $(\boldsymbol{\Phi}_{K,F}(\mathbb{w}_h, \mathbb{r}_h))_{K \in \mathcal{K}_h, F \in \mathcal{F}_K}$ with $\boldsymbol{\Phi}_{K,F}(\mathbb{w}_h, \mathbb{r}_h) = (\Phi_{K,F,i}(\mathbb{w}_h, \mathbb{r}_h))_{1 \leqslant i \leqslant d}$ and $(\phi_F(\mathbb{w}_h))_{F \in \mathcal{F}_{\mathcal{K}_h}}$ such that (the expression for the vectors $\boldsymbol{y}_{F',F}^K$ is provided in Proposition 22)

$$\Phi_{K,F,i}(\mathbb{w}_h, \mathbb{r}_h) := \sum_{F' \in \mathcal{F}_K} |K_{F'}| \left(\boldsymbol{G}_{K_{F'}}(\mathbb{w}_{h,i}) + r_K \boldsymbol{e}_i \right) \cdot \boldsymbol{y}_{F',F}^K, \qquad \phi_F(\mathbb{w}_h) := |F| \sum_{j=1}^d w_{F,j} n_{F,j},$$

there holds,

$$
\begin{aligned}
a_h(\boldsymbol{w}_h, \boldsymbol{v}_h) + b_h(\boldsymbol{v}_h, r_h) &= \sum_{i=1}^{d} \sum_{K \in \mathcal{K}_h} \sum_{F \in \mathcal{F}_K} \Phi_{K,F,i}(\mathbb{w}_h, \mathbb{r}_h)(v_{F,i} - v_{K,i}), \\
-b_h(\boldsymbol{w}_h, q_h) &= \sum_{F \in \mathcal{F}_{\mathcal{K}_h}} \phi_F(\mathbb{w}_h) [\![\mathbb{q}_h]\!]_F,
\end{aligned}
\tag{57}
$$

where a_h and b_h are defined as in Section 4.3.1 and, with a slight abuse in notation, we have set for all $F \in \mathcal{F}_{\mathcal{K}_h}$, $[\![\mathbb{q}_h]\!]_F := [\![q_h]\!]_F$. Approximating the right-hand side as $\sum_{i=1}^{d} \sum_{K \in \mathcal{K}_h} |K| \, f_i(\boldsymbol{x}_K) v_{K,i}$ in (54), and proceeding as in Section 4.2.4, one can prove that for every interface $F \in \mathcal{F}^{\mathrm{i}}_{\mathcal{K}_h}$ such that $F \subset \partial K_1 \cap \partial K_2$ there holds $\boldsymbol{\Phi}_{K_1,F}(\mathbb{u}_h, \mathbb{p}_h) = -\boldsymbol{\Phi}_{K_2,F}(\mathbb{u}_h, \mathbb{p}_h)$, where $\mathbb{u}_h, \mathbb{p}_h$ are such that $\boldsymbol{u}_h := \mathfrak{R}_h(\mathbb{u}_h)$ and $p_h := \mathfrak{R}_h(\mathbb{p}_h)$ with $(\boldsymbol{u}_h, p_h) \in \boldsymbol{U}_h \times P_h$ solution of (54). Moreover, the mass flux $\phi_F(\mathbb{u}_h)$ is single-valued, and therefore conservative.

Link with the Crouzeix–Raviart solution on matching simplicial meshes Assume $\mathcal{K}_h$ matching simplicial. The classical Crouzeix–Raviart/$\mathbb{P}^0_d$ method consists in finding $(\hat{\boldsymbol{u}}_h, \hat{p}_h) \in \hat{\boldsymbol{U}}_h \times P_h$ with $\hat{\boldsymbol{U}}_h := \mathbb{CR}_0(\mathcal{K}_h)^d$ such that

$$
a_h(\hat{\boldsymbol{u}}_h, \boldsymbol{v}_h) + b_h(\boldsymbol{v}_h, \hat{p}_h) - b_h(\hat{\boldsymbol{u}}_h, q_h) = (\boldsymbol{f}, \boldsymbol{v}_h)_{L^2(\Omega)^d} \qquad \forall (\boldsymbol{v}_h, q_h) \in \hat{\boldsymbol{U}}_h \times P_h. \tag{58}
$$

Then, proceeding as in Section 4.2.4, one can easily show that the solution to (58) can be recovered replacing the right-hand side of (54) by $(\boldsymbol{f}, \mathcal{I}_h^{\mathbb{CR}}(\boldsymbol{v}_h))_{L^2(\Omega)^d}$.

4.3.3 Large irrotational body forces

We close this section by discussing a general modification applicable to any suitable discretization of the Stokes equations that allows a proper treatment of large irrotational body forces, and we apply it to the method (54).We assume here that the following Helmholtz decomposition of the volumetric body forces in (52) is available:

$$
\boldsymbol{f} = \boldsymbol{\Psi} - \boldsymbol{\nabla} \varphi, \tag{59}
$$

where $\boldsymbol{\Psi} \in \boldsymbol{H}_0(\mathrm{div}; \Omega) := \{\boldsymbol{v} \in \boldsymbol{H}(\mathrm{div}; \Omega) \mid \boldsymbol{\nabla} \cdot \boldsymbol{v} = 0\}$ is a solenoidal vector field and $\varphi \in H^1(\Omega) \cap L^2_0(\Omega)$ is a scalar potential. It has to be noted that the decomposition (59) is not always easy to obtain.The weak formulation of problem (52) with right-hand side given by (59) reads: Find $(\boldsymbol{u}, p) \in \boldsymbol{U} \times P$ such that

$$
a(\boldsymbol{u}, \boldsymbol{v}) + b(\boldsymbol{v}, p) - b(\boldsymbol{u}, q) = l(\boldsymbol{v}) \qquad \forall (\boldsymbol{v}, q) \in \boldsymbol{U} \times P, \tag{60}
$$

with bilinear forms a and b defined as in Section 4.3.1 and $l(\boldsymbol{v}) := (\boldsymbol{\Psi}, \boldsymbol{v})_{L^2(\Omega)^d} - b(\boldsymbol{v}, \varphi)$. Denoting by $(\boldsymbol{u}_{\boldsymbol{\Psi}}, p_{\boldsymbol{\Psi}})$ the solution to (60) with $\varphi \equiv 0$ (no irrotational body forces), there holds

$$
\boldsymbol{u} = \boldsymbol{u}_{\boldsymbol{\Psi}}, \qquad p = p_{\boldsymbol{\Psi}} - \varphi. \tag{61}
$$

As pointed out in [27], mimicking or approaching property (61) at the discrete level is a key ingredient to obtain an accurate approximation of the velocity field for large values of $\|\varphi\|_{H^1(\Omega)}$. We hence consider the following approximation to (60): Find $(\boldsymbol{u}_h, p_h) \in \boldsymbol{U}_h \times P_h$ such that

$$
a_h(\boldsymbol{u}_h, \boldsymbol{v}_h) + b_h(\boldsymbol{v}_h, p_h) - b_h(\boldsymbol{u}_h, q_h) = l_h(\boldsymbol{v}_h) \qquad \forall (\boldsymbol{v}_h, q_h) \in \boldsymbol{U}_h \times P_h, \tag{62}
$$

with bilinear forms a_h and b_h defined as in Section 4.3.1 and $l_h(\boldsymbol{v}_h) := (\boldsymbol{\Psi}, \boldsymbol{v}_h)_{L^2(\Omega)^d} - b_h(\boldsymbol{v}_h, \Pi^0_h \varphi)$. The sole difference with respect to (54) lies in the treatment of the source term, which is designed so that the following property holds true.

Proposition 28 (Discrete counterpart of property (61))**.** *Denote by* $(\boldsymbol{u}_{\boldsymbol{\Psi},h}, p_{\boldsymbol{\Psi},h})$ *the solution to problem* (62) *with* $\varphi \equiv 0$*. There holds*

$$\boldsymbol{u}_h = \boldsymbol{u}_{\boldsymbol{\Psi},h}, \qquad p_h = p_{\boldsymbol{\Psi},h} - \Pi_h^0 \varphi.$$

The following result shows that the velocity approximation is not affected by the irrotational part of the source term.

Theorem 29 (Error estimate for (62))**.** *Assume* $\boldsymbol{u} \in \boldsymbol{U} \cap H^2(\Omega)^d$ *and* $p \in P \cap H^1(\Omega)$*. Then, there holds with real numbers* $C_1 > 0$ *and* $C_2 > 0$ *independent of the meshsize, of* $\boldsymbol{u}$*, and of* p*, but depending on the mesh regularity parameters and on* Ω*,*

$$\|\boldsymbol{u} - \boldsymbol{u}_h\|_{\boldsymbol{U}} \leqslant C_1 h \mathcal{N}_{\mathrm{sto}}(\boldsymbol{u}_{\boldsymbol{\Psi}}, p_{\boldsymbol{\Psi}}), \qquad \|p - p_h\|_P \leqslant C_2 h \left(\mathcal{N}_{\mathrm{sto}}(\boldsymbol{u}_{\boldsymbol{\Psi}}, p_{\boldsymbol{\Psi}}) + \|\varphi\|_{H^1(\Omega)}\right).$$

Proof. Using Theorem 27 for the approximate solution to problem (60) with $\varphi \equiv 0$, we infer $\|\boldsymbol{u}_{\boldsymbol{\Psi}} - \boldsymbol{u}_{\boldsymbol{\Psi},h}\|_{\boldsymbol{U}} + \|p_{\boldsymbol{\Psi}} - p_{\boldsymbol{\Psi},h}\|_P \leqslant C h \mathcal{N}_{\mathrm{sto}}(\boldsymbol{u}_{\boldsymbol{\Psi}}, p_{\boldsymbol{\Psi}})$, where $C > 0$ has the same dependencies as C_1 and C_2. The estimate for $\|\boldsymbol{u} - \boldsymbol{u}_h\|_{\boldsymbol{U}}$ is an immediate consequence of (61) and Proposition 28. To estimate $\|p - p_h\|_P$ we invoke again (61) and Proposition 28 to infer $\|p - p_h\|_P \leqslant \|p_{\boldsymbol{\Psi}} - p_{\boldsymbol{\Psi},h}\|_P + \|\varphi - \Pi_h^0 \varphi\|_P$, and conclude using the above estimate for $\|p_{\boldsymbol{\Psi}} - p_{\boldsymbol{\Psi},h}\|_P$ and the approximation properties of the L^2-orthogonal projector. □

In practice, one can solve the problem with $\varphi \equiv 0$ and then post-process the pressure approximation according to Proposition 28.To check the theoretical results, we consider a numerical example based on the following manufactured solution on the unit square domain $\Omega := (0,1)^2$:

$$u_1 = -e^{x_1}(x_2 \cos(x_2) + \sin(x_2)), \quad u_2 = e^{x_1} x_2 \sin(x_2), \quad p_{\boldsymbol{\Psi}} = 2\exp(x_1)\sin(x_2) - C,$$

with C such that $p_{\boldsymbol{\Psi}}$ has zero-mean on Ω, $\boldsymbol{\Psi} \equiv \boldsymbol{0}$, and a potential $\varphi = \chi \sin(2\pi x_1)\sin(2\pi x_2)$, where χ is a positive parameter that allows to adjust its intensity. In Figure 5 we compare the numerical results obtained with the modified right-hand side (62) to those obtained with a standard treatment (54) for the triangular and hexagonal mesh families depicted in Figure 3a and 3d, respectively. The results confirm that a standard treatment of the right-hand side does not yield satisfactory results.

A Mimicking the properties of the lowest-order Raviart–Thomas space on general meshes

In the spirit of Section 3.1, it is possible to extend two classical properties of the lowest-order Raviart–Thomas space to general polygonal or polyhedral meshes, namely (i) the (full) continuity of normal components of discrete functions at interfaces and (ii) the existence of an interpolator which preserves the mean value of the divergence inside each element. Since the construction as well as the proofs are similar to the ones presented in Section 3, only the main points are detailed. For a matching simplicial mesh, we introduce the broken polynomial space

$$\mathbb{RT}_d^0(\mathcal{K}_h) := \mathbb{P}_d^0(\mathcal{K}_h)^d + \boldsymbol{x}\mathbb{P}_d^0(\mathcal{K}_h). \tag{63}$$

The standard lowest-order Raviart–Thomas space is the subspace of $\boldsymbol{H}(\mathrm{div};\Omega)$ of functions belonging to $\mathbb{RT}_d^0(\mathcal{K}_h)$. To perform a similar construction on general polygonal or polyhedral meshes, we consider the following space of DOFs, composed of vector cell unknowns and scalar face unknowns associated to the normal component of the discrete vector field:

$$\mathbb{V}_h := \{\mathbb{v}_h = ((\boldsymbol{v}_K \in \mathbb{R}^d)_{K \in \mathcal{K}_h}, (v_F^n \in \mathbb{R})_{F \in \mathcal{F}_{\mathcal{K}_h}})\}.$$

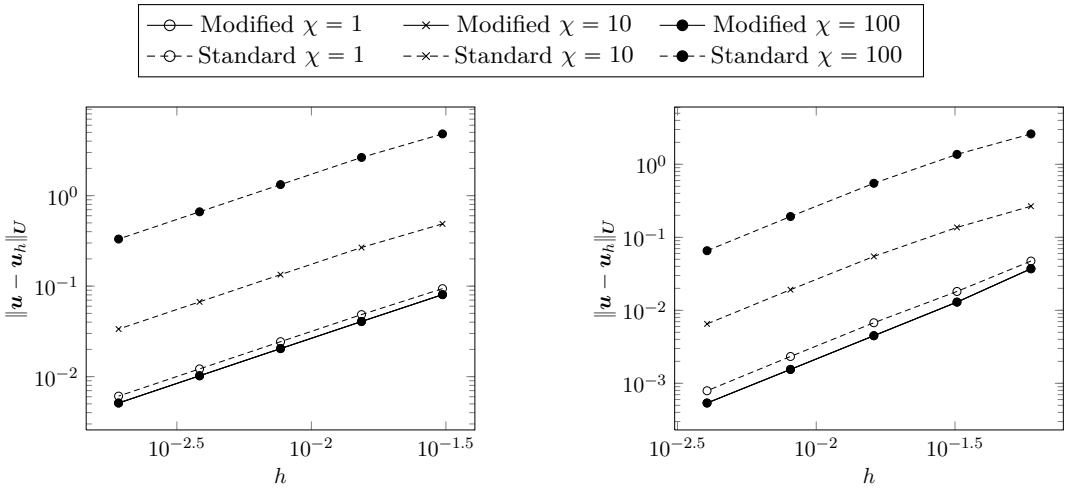

(a) Triangular mesh family

(b) Hexagonal mesh family

Figure 5: Effect of the treatment of the right-hand side (62) (Modified, solid lines) vs. (54) (Standard, dashed lines) when large irrotational volumetric forces are present. For a standard treatment of the right-hand side, the error on the velocity increases with χ.

As it is the case for the extension of the Crouzeix–Raviart space discussed in Section 3, cell unknowns are used to define a piecewise constant subgrid correction on the pyramidal submesh. The main difference with respect to the construction of Section 3 is that we now define an isotropic instead of a full gradient operator. More specifically, we introduce the operator $\mathfrak{G}_h : \mathbb{V}_h \to \mathbb{P}_d^0(\mathcal{P}_h)$ which realizes the mapping $\mathbb{v}_h \mapsto \mathfrak{G}_h(\mathbb{v}_h)$ with

$$\mathfrak{G}_h(\mathbb{v}_h)_{|K_F} = G_K(\mathbb{v}_h) + R_{K_F}(\mathbb{v}_h), \qquad \forall K \in \mathcal{K}_h,\, \forall F \in \mathcal{F}_K,$$

where

$$G_K(\mathbb{v}_h) := \frac{1}{d\,|K|} \sum_{F \in \mathcal{F}_K} |F|\, v_F^n \boldsymbol{n}_F \cdot \boldsymbol{n}_{K,F},\ R_{K_F}(\mathbb{v}_h) := \frac{\eta}{d_{K,F}} (v_F^n \boldsymbol{n}_F - \boldsymbol{v}_K - G_K(\mathbb{v}_h)(\overline{\boldsymbol{x}}_F - \boldsymbol{x}_K)) \cdot \boldsymbol{n}_{K,F}, \tag{64}$$

and $\eta > 0$ is a user-dependent parameter. Extending the definition (63), we introduce the reconstruction operator $\mathfrak{R}_h : \mathbb{V}_h \to \mathbb{RT}_d^0(\mathcal{P}_h)$ which realizes the mapping $\mathbb{v}_h \mapsto \mathfrak{R}_h(\mathbb{v}_h)$ with

$$\mathfrak{R}_h(\mathbb{v}_h)_{|K_F}(\boldsymbol{x}) = \boldsymbol{v}_K + \mathfrak{G}_h(\mathbb{v}_h)_{|K_F}(\boldsymbol{x} - \boldsymbol{x}_K), \qquad \forall K_F \in \mathcal{P}_h,\, \forall \boldsymbol{x} \in K_F. \tag{65}$$

Unlike (10), there holds for all $K \in \mathcal{K}_h$, $\boldsymbol{v}_K = \mathfrak{R}_h(\mathbb{v}_h)(\boldsymbol{x}_K)$, i.e., the cell unknown can now be interpreted as the value of the reconstruction at the cell center. This is a consequence of selecting the cell center as a starting point in (65). We consider the discrete space

$$\mathfrak{RT}(\mathcal{K}_h) := \mathfrak{R}_h(\mathbb{V}_h).$$

Lemma 30 ($\boldsymbol{H}(\mathrm{div};\Omega)$-conformity)**.** *Assume $\eta = 1$ in (64). Then, for all $\boldsymbol{v}_h \in \mathfrak{RT}(\mathcal{K}_h)$ and all $F \in \mathcal{F}^{\mathrm{i}}_{\mathcal{P}_h}$, there holds for all $\boldsymbol{x} \in F$,*

$$[\![\boldsymbol{v}_h]\!]_F(\boldsymbol{x}) \cdot \boldsymbol{n}_F = 0.$$

Proof. Let $\boldsymbol{v}_h \in \mathfrak{RT}(\mathcal{K}_h)$ with $\boldsymbol{v}_h = \mathfrak{R}_h(\mathbb{v}_h)$, $F \in \mathcal{F}^{\mathrm{i}}_{\mathcal{P}_h}$, and $\boldsymbol{x} \in F$. We distinguish two cases.
(i) $F \in \mathcal{F}^{\mathrm{i}}_{\mathcal{K}_h}$ is an interface of the primal mesh $\mathcal{K}_h$ such that $F \subset \partial K_1 \cap \partial K_2$. For $i \in \{1, 2\}$ let, for the sake of brevity, $G_i := G_{K_i}(\mathbb{v}_h)$, $R_i := R_{K_i F}(\mathbb{v}_h)$, $d_i := d_{K_i,F}(\boldsymbol{n}_{K_i,F} \cdot \boldsymbol{n}_F)$, and

$$\alpha_i := R_i(\boldsymbol{x} - \boldsymbol{x}_{K_i}) \cdot \boldsymbol{n}_F = R_i d_i = \eta\,(v_F^n \boldsymbol{n}_F - \boldsymbol{v}_{K_i} - G_i(\overline{\boldsymbol{x}}_F - \boldsymbol{x}_{K_i})) \cdot \boldsymbol{n}_F,$$

where we have used the fact that $\boldsymbol{x} \in F$ to infer $(\boldsymbol{x} - \boldsymbol{x}_{K_i})\cdot\boldsymbol{n}_F = d_i$ and the fact that $\boldsymbol{n}_F = \boldsymbol{n}_{K_1,F} = -\boldsymbol{n}_{K_2,F}$ to infer $(\boldsymbol{n}_{K_i,F}\cdot\boldsymbol{n}_F)\,\boldsymbol{n}_{K_i,F} = \boldsymbol{n}_F$. Algebraic manipulations yield

$$\alpha_1 - \alpha_2 = -\eta\left[(\boldsymbol{v}_{K_1} - \boldsymbol{v}_{K_2})\cdot\boldsymbol{n}_F + G_1 d_1 - G_2 d_2\right].$$

Using the previous relation in the definition of the jump at $\boldsymbol{x} \in F$ it is inferred,

$$\begin{aligned}
[\![\boldsymbol{v}_h]\!]_F(\boldsymbol{x})\cdot\boldsymbol{n}_F &= \boldsymbol{v}_{h|K_{1F}}(\boldsymbol{x})\cdot\boldsymbol{n}_F - \boldsymbol{v}_{h|K_{2F}}(\boldsymbol{x})\cdot\boldsymbol{n}_F \\
&= (\boldsymbol{v}_{K_1} - \boldsymbol{v}_{K_2})\cdot\boldsymbol{n}_F + G_1 d_1 - G_2 d_2 + \alpha_1 - \alpha_2 \\
&= (1-\eta)\left[(\boldsymbol{v}_{K_1} - \boldsymbol{v}_{K_2})\cdot\boldsymbol{n}_F + G_1 d_1 - G_2 d_2\right].
\end{aligned}$$

As a consequence, the jump vanishes provided $\eta = 1$.
(ii) $F \in \mathcal{F}^{\mathsf{i}}_{\mathcal{P}_h} \backslash \mathcal{F}^{\mathsf{i}}_{\mathcal{K}_h}$ is a lateral pyramidal face such that there exist a unique element $K \in \mathcal{K}_h$ and two faces F_1, $F_2 \in \mathcal{F}_K$ such that $F \subset \partial K_{F_1} \cap \partial K_{F_2}$ (cf. Figure 2a). There holds, letting for the sake of brevity $R_i := R_{K_{F_i}}(\mathbb{v}_h)$, $i \in \{1, 2\}$,

$$[\![\boldsymbol{v}_h]\!]_F(\boldsymbol{x})\cdot\boldsymbol{n}_F = \boldsymbol{v}_{h|K_{F_1}}(\boldsymbol{x})\cdot\boldsymbol{n}_F - \boldsymbol{v}_{h|K_{F_2}}(\boldsymbol{x})\cdot\boldsymbol{n}_F = (R_1 - R_2)(\boldsymbol{x} - \boldsymbol{x}_K)\cdot\boldsymbol{n}_F = 0,$$

since $(\boldsymbol{x} - \boldsymbol{x}_K)$ and $\boldsymbol{n}_F$ are orthogonal by definition. This concludes the proof. □

Remark 31 (Role of η in the proof of Lemma 30)**.** *Unlike Lemma 8, the parameter η is here used to enforce the continuity of the normal component across the interfaces of the primal mesh rather than across lateral pyramidal faces.*

Let $\mathcal{I}_h^{\mathfrak{RT}} : \boldsymbol{H}(\mathrm{div};\Omega) \to \mathfrak{RT}(\mathcal{K}_h)$ be such that $\mathcal{I}_h^{\mathfrak{RT}}(\boldsymbol{v}) := \mathfrak{R}_h(\mathbb{v}_h)$ with

$$\mathbb{V}_h \ni \mathbb{v}_h = ((\Pi_h^1 \boldsymbol{v}(\boldsymbol{x}_K))_{K\in\mathcal{K}_h},\ (\langle\boldsymbol{v}\rangle_F\cdot\boldsymbol{n}_F)_{F\in\mathcal{F}_{\mathcal{K}_h}}).$$

The following result summarizes the most relevant approximation properties of $\mathcal{I}_h^{\mathfrak{RT}}$. The proof is omitted as it closely resembles that of Lemma 10.

Lemma 32 (Approximation in $\mathfrak{RT}(\mathcal{K}_h)$)**.** *For all $\eta > 0$ in (64) and all $\boldsymbol{v} \in \boldsymbol{H}(\mathrm{div};\Omega)$ there holds with $\boldsymbol{v}_h := \mathcal{I}_h^{\mathfrak{RT}}(\boldsymbol{v})$,*

$$D_h(\boldsymbol{v}_h) = \Pi_h^0(\boldsymbol{\nabla}\cdot\boldsymbol{v}).$$

Moreover, there exists a real $C > 0$ independent of the meshsize such that, for all $h \in \mathcal{H}$, all $K \in \mathcal{K}_h$, and all $\boldsymbol{v} \in \boldsymbol{H}(\mathrm{div};\Omega) \cap \boldsymbol{H}^1(\mathrm{div};\mathcal{K}_h)$ with $\boldsymbol{v}_h := \mathcal{I}_h^{\mathfrak{RT}}(\boldsymbol{v})$, there holds

$$\|\boldsymbol{v} - \boldsymbol{v}_h\|_{L^2(K)^d} + \|\boldsymbol{\nabla}\cdot\boldsymbol{v} - D_h(\boldsymbol{v}_h)\|_{L^2(K)} \leqslant C h_K \left(|\boldsymbol{v}|_{H^1(K)^d} + |\boldsymbol{\nabla}\cdot\boldsymbol{v}|_{H^1(K)}\right).$$

Remark 33 (The matching simplicial case)**.** *When $\mathcal{K}_h$ is matching simplicial, in the spirit of Proposition 9, we can prove that the lowest-order Raviart–Thomas space is a subspace of $\mathfrak{RT}(\mathcal{K}_h)$. We also emphasize that the assumption $\eta = 1$ in Lemma 30 is mandatory for the continuity of normal values at interfaces also in the matching simplicial case.*

References

[1] G. Allaire. *Analyse numérique et optimisation.* Les éditions de l'École Polytechnique, Palaiseau, 2009.

[2] D. N. Arnold, F. Brezzi, and J. Douglas. PEERS: A new mixed finite element for plane elasticity. *Japan Journal of Industrial and Applied Mathematics*, 1(2):347–367, 1984.

[3] L. Beirão da Veiga. A mimetic discretization method for linear elasticity. *M2AN Math. Model. Numer. Anal.*, 44(2):231–250, 2010.

[4] L. Beirão da Veiga, F. Brezzi, and L. D. Marini. Virtual elements for linear elasticity problems. *SIAM J. Numer. Anal.*, 51(2):794–812, 2013.

[5] L. Beirão da Veiga, V. Gyrya, K. Lipnikov, and G. Manzini. Mimetic finite difference method for the Stokes problem on polygonal meshes. *J. Comput. Phys.*, 228(19):7215–7232, 2009.

[6] L. Beirão da Veiga, K. Lipnikov, and G. Manzini. Error analysis for a mimetic discretization for the steady Stokes problem on polyhedral meshes. *SIAM J. Numer. Anal.*, 48(4):1419–1443, 2010.

[7] S. C. Brenner. Korn's inequalities for piecewise H^1 vector fields. *Math. Comp.*, 73(247):1067–1087, 2004.

[8] S. C. Brenner and L. R. Scott. *The mathematical theory of finite element methods*, volume 15 of *Texts in Applied Mathematics*. Springer, New York, third edition, 2008.

[9] S. C. Brenner and L.-Y. Sung. Linear finite element methods for planar linear elasticity. *Math. Comp.*, 59(200):321–338, 1992.

[10] F. Brezzi and M. Fortin. *Mixed and hybrid finite element methods*, volume 15 of *Springer Series in Computational Mathematics*. Springer-Verlag, New York, 1991.

[11] F. Brezzi, K. Lipnikov, and M. Shashkov. Convergence of the mimetic finite difference method for diffusion problems on polyhedral meshes. *SIAM J. Numer. Anal.*, 43(5):1872–1896, 2005.

[12] F. Brezzi, K. Lipnikov, M. Shashkov, and V. Simoncini. A new discretization methodology for diffusion problems on generalized polyhedral meshes. *Comput. Methods Appl. Mech. Engrg.*, 196(37–40):3682–3692, 2007.

[13] F. Brezzi, K. Lipnikov, and V. Simoncini. A family of mimetic finite difference methods on polygonal and polyhedral meshes. *Math. Mod. Meths. Appli. Sci. (M3AS)*, 15(10):1533–1551, 2005.

[14] K. S. Chavan, B. P. Lamichhane, and B. I. Wohlmuth. Locking-free finite element methods for linear and nonlinear elasticity in 2D and 3D. *Comput. Methods Appl. Mech. Engrg.*, 196:4075–4086, 2007.

[15] M. Crouzeix and P.-A. Raviart. Conforming and nonconforming finite element methods for solving the stationary Stokes equations. *RAIRO Modél. Math. Anal. Num.*, 7(3):33–75, 1973.

[16] D. A. Di Pietro. Cell centered Galerkin methods for diffusive problems. *M2AN Math. Model. Numer. Anal.*, 46(1):111–144, 2012.

[17] D. A. Di Pietro and A. Ern. *Mathematical aspects of discontinuous Galerkin methods*, volume 69 of *Mathématiques & Applications*. Springer-Verlag, Berlin, 2011.

[18] D. A. Di Pietro, J.-M. Gratien, and C. Prud'homme. A domain-specific embedded language in C++ for lowest-order discretizations of diffusive problems on general meshes. *BIT Numerical Mathematics*, 53(1):111–152, 2013.

[19] D. A. Di Pietro and S. Nicaise. A locking-free discontinuous Galerkin method for linear elasticity in locally nearly incompressible heterogeneous media. *App. Num. Math.*, 63:105–116, 2013.

[20] J. Droniou and R. Eymard. A mixed finite volume scheme for anisotropic diffusion problems on any grid. *Numer. Math.*, 105(1):35–71, 2006.

[21] J. Droniou and R. Eymard. Study of the mixed finite volume method for Stokes and Navier–Stokes equations. *Numer. Methods for Partial Differential Equations*, 25(1):137–171, 2009.

[22] J. Droniou, R. Eymard, T. Gallouët, and R. Herbin. A unified approach to mimetic finite difference, hybrid finite volume and mixed finite volume methods. *Math. Mod. Meths. Appli. Sci. (M3AS)*, 20(2):265–295, 2010.

[23] T. Dupont and R. Scott. Polynmomial approximation of functions in Sobolev spaces. *Math. Comp.*, 34(150):441–463, 1980.

[24] A. Ern and J.-L. Guermond. *Theory and practice of finite elements*, volume 159 of *Applied Mathematical Sciences*. Springer-Verlag, New York, 2004.

[25] R. Eymard, T. Gallouët, and R. Herbin. Discretization of heterogeneous and anisotropic diffusion problems on general nonconforming meshes. SUSHI: a scheme using stabilization and hybrid interfaces. *IMA J. Num. Anal.*, 30(4):1009–1043, 2010.

[26] R. S. Falk. Nonconforming finite element methods for the equations of linear elasticity. *Math. Comp.*, 57(196):529–550, 1991.

[27] K. J. Galvin, A. Linke, L. G. Rebholz, and N. E. Wilson. Stabilizing poor mass conservation in incompressible flow problems with large irrotational forcing and application to thermal convection. *Comput. Methods Appl. Mech. Engrg.*, 237–240:166–176, 2012.

[28] P. Hansbo and M. G. Larson. Discontinuous Galerkin methods for incompressible and nearly incompressible elasticity by Nitsche's method. *Comput. Methods Appl. Mech. Engrg.*, 191(17–18):1895–1908, 2002.

[29] P. Hansbo and M. G. Larson. Discontinuous Galerkin and the Crouzeix–Raviart element: application to elasticity. *M2AN Math. Model. Numer. Anal.*, 37(1):63–72, 2003.

[30] B. P. Lamichhane and E. P. Stephan. A symmetric mixed finite element method for nearly incompressible elasticity based on biorthogonal systems. *Numer. Methods for Partial Differential Equations*, 28(4):1336–1353, 2012.

[31] R. Stenberg. A family of mixed finite elements for the elasticity problem. *Numer. Math.*, 53:513–538, 1988.

[32] G. Strang. Variational crimes in the finite element method. In A. Aziz, editor, *The Mathematical Foundations of the Finite Element Method with Applications to Partial Differential Equations*. Academic Press, New York, 1972.

[33] M. Vogelius. An analysis of the p-version of the finite element method for nearly incompressible materials. Uniformly valid, optimal error estimates. *Numer. Math.*, 41:39–53, 1983.

[34] M. Vohralík and B. I. Wohlmuth. From face to element unknowns by local static condensation with application to nonconforming finite elements. *Comput. Methods Appl. Mech. Engrg.*, 253:517–529, 2013.

[35] M. Vohralík and B. I. Wohlmuth. Mixed finite element methods: implementation with one unknown per element, local flux expressions, positivity, polygonal meshes, and relations to other methods. *Math. Mod. Meths. Appli. Sci. (M3AS)*, 23, 2013. Published online. DOI 10.1142/S0218202512500613.